European Journal of Operational Research 309 (2023) 1218–1236

Contents lists available at ScienceDirect

European Journal of Operational Research

journal homepage: www.elsevier.com/locate/ejor

Innovative Applications of O.R.

Randomization and the valuation of guaranteed minimum death benefits

Griselda Deelstra[a], Peter Hieber[b,*]

[a] Department of Mathematics, Université Libre de Bruxelles, Boulevard du Triomphe, Brussels 1050, Belgium
[b] Department of Actuarial Science, Faculty of Business and Economics, University of Lausanne, Lausanne 1015, Switzerland

ARTICLE INFO

Article history:
Received 12 May 2022
Accepted 27 January 2023
Available online 2 February 2023

JEL classification:
G11
G22
G23

Keywords:
Risk analysis
Variable annuities
Erlangization
Regime switching
Phase-type distributions

ABSTRACT

In this article, we focus on death-linked contingent claims (GMDBs) paying a random financial return at a random time of death in the general case where financial returns follow a regime switching model with two-sided phase-type jumps. We approximate the distribution of the remaining lifetime by either a series of Erlang distributions or a Laguerre series expansion, whose capability to fit the tail of the observed mortality data turns out to be much better than the commonly used series of exponential distributions.

More precisely, we develop a Laurent series expansion of the discounted Laplace transform of the subordinated process at an Erlang distributed time, which leads to explicit formulae for European-type GMDB as well as related risk measures such as the Value-at-Risk (VaR) and the Conditional-Tail-Expectation (CTE). We further concentrate upon path-dependent GMDBs with lookback features like dynamic fund protection or dynamic withdrawal benefits, by relying on a Sylvester equation approach. The advantage of our approaches is that our results are of semi-closed form, avoiding numerical Fourier inversion or Monte-Carlo simulation, leading to fast evaluation. This is necessary in risk-management, in particularly for nested simulation in the framework of Solvency II. Several numerical experiments are included.

Our results have implications beyond life-insurance and GMDBs, namely in all situations where randomization or Erlangization replaces known quantities, like, for example, model parameters, by random variables. In Finance, it is for example well-known that a random maturity time leads to much more convenient valuation formulas that well approximate its non-random counterpart.

1. Introduction and motivation

In many disciplines, risk analysis and optimal control is based on time-changed Markov processes, accounting for the fact that – often – not only the underlying process itself is random but also the time it is observed (see, e.g., Hieber & Scherer, 2012, Cui, Kirkby, & Nguyen, 2019 and the references therein). This is also the case in insurance, where contract payoffs depend on a financial risk process while claim dates are random events like death or the occurence of a claim or natural catastrophe. While the results in this article can have many applications in different disciplines, the focus is on death-linked insurance products, i.e. Guaranteed Minimum Death Benefits (GMDB) that pay a certain (random) financial payoff at the time of death, a feature often embedded in variable annuities. For the two sources of risk, we try to be very general and flexible: The underlying financial return process follows a regime switching Brownian motion with two-sided phase-type jumps (see also Asmussen, 2003, Jiang & Pistorius, 2008) while the distribution of the random payment times can be approximated by a series expansion. One of the pioneering works on regime switching models is Hamilton (1989) suggesting that financial models should account for the cyclical pattern of boom and recession observed in many financial time series. The idea of such models is that model parameters may depend on a (typically small) number of "phases" modelled by a Markov process. Just to mention few examples: These processes turn out to be convenient to discuss optimal consumption and control in Finance (see, e.g., Korn, Melnyk, & Seifried, 2017, Jin, Liu, & Yang, 2020), pension fund modeling in Insurance (see, e.g., Hainaut, 2014) or cyclical patterns in temperature modeling (see, e.g., Elias, Wahab, & Fang, 2014).

The distribution of a random payment date can be approximated by a Laguerre series expansion that is dense in the class of

* Corresponding author.
E-mail addresses: peter.hieber@unil.ch, hieber@tum.de (P. Hieber).

https://doi.org/10.1016/j.ejor.2023.01.059

L^2-distributions (see e.g. Zhang & Yong, 2019) or by combinations of Erlang distributions. Technically, such Laguerre series expansions can be linked to Erlang distributions. An Erlang random variable $\tau_{N,\mu}$ with parameters $N \in \mathbb{N}$ and $\mu > 0$ has the same distribution as the sum of N independent exponential random variables. It has density function

$$f_{\tau_{N,\mu}}(t) = \frac{\mu(\mu t)^{N-1}}{(N-1)!} e^{-\mu t}, \quad t > 0. \tag{1}$$

Erlang distributions inherit many desirable features from the exponential distribution that is obtained as the special case $N = 1$. Interestingly, a contingent claim that is due at a random exponential time $\tau_{1,\mu}$ can often be priced much easier than its fixed-time counterpart. The reason for this is that in the class of regime switching Brownian motion with two-sided phase-type jumps, it is often the Laplace transform of the logarithmic returns that is known analytically. For a fixed-time contingent claim, values or higher-order moments require a numerical Laplace inversion algorithm. In contrast, for a random contingent claim, these quantities can just be expressed in terms of the known Laplace transform. This was one reason why, in Finance, the idea appeared to “randomize” the payment date of options, an approach named “Carr’s randomization”, “Canadization” or “Erlangization”.

The suggestion is to approximate the option’s fixed maturity time T by an Erlang distributed random variable with mean T and standard deviation $T/\sqrt{N}$ for $N \in \mathbb{N}$, i.e. choose $\mu = T/N$ in (1). If N is sufficiently high, this well approximates the original problem with constant maturity T. With this modification, one can typically approximate the finite horizon valuation problem by a (modified) infinite horizon problem that is much easier to solve. An example is the pricing of American options where randomization leads to piecewise constant exercise boundaries. The pioneering work in this direction is (Carr, 1998); for related applications to insurance and risk theory we refer to, e.g., Asmussen & Albrecher (2010), Chapter IX.8. In insurance applications, however, payment dates of GMDBs are per se random. There is no necessity to approximate a fixed payment date, that is we can use two-parametric Erlang distributions with small values of N. Being dense in the class of L^2-distributions, combinations of these Erlang random variables allow to well approximate any death time distribution (or, more generally, any distribution of a random observation time).

This article establishes the links between (on first sight) quite different strands of literature, namely Erlangization in Finance (e.g. Carr, 1998, Deelstra, Latouche, & Simon, 2020), the discounted density approach for GMDB valuation (e.g. Gerber, Shiu, & Yang, 2012; Gerber, Shiu, & Yang, 2015, Zhang & Yong, 2019) and the matrix Wiener-Hopf factorisation (e.g. Jiang & Pistorius, 2008). Closest to this article is Gerber et al. (2012, 2015) – pioneering work on GMDB valuation that has been extended in several directions, i.e. piecewise constant forces of mortality (Liang, Tsai, & Lu, 2016), regime-switching jumps and volatility (Ai & Zhang, 2022; Cui, Kirkby, & Nguyen, 2017; Siu, Yam, & Yang, 2015; Wang, Zhang, & Yu, 2021; Zhang, Yong, & Yu, 2021), different types of payoffs (Kirkby & Nguyen, 2021; Zhang & Yong, 2019) and different types of random time approximations (Zhang & Yong, 2019).

We generalize these existing works to a more flexible financial market model including a regime-dependent interest rate and two-sided phase-type jumps. This model class is very general and allows to well approximate stochastic volatility or heavier, power-type tails of the jump distributions, see, e.g., Mijatović & Pistorius (2011), Cai & Kou (2011). This is useful also for stress testing or risk management. Second, we do not rely on Fourier techniques and instead provide computationally very convenient techniques for valuation and the computation of higher-order moments that are either closed-form or require solely to solve a certain type of affine matrix equation called Sylvester equation. We demonstrate that this is usually significantly faster and easier to implement than Fourier or Laplace inversion algorithms. Given the complexity of the models used, Fourier-based algorithms are typically computationally more efficient than Monte-Carlo simulations (see, e.g., Huang, Zhu, & Ruan, 2014, Benth, Deelstra, & Kozpinar, 2021, Ai & Zhang, 2022). The computation of solvency capital requirements in insurance companies requires fast and accurate valuations in base-case and stress scenarios. This typically requires the annual re-valuation of the whole insurance portfolio with its embedded options in different economic scenarios. If these re-valuations are based on Monte-Carlo, one typically faces the problem of so-called nested-simulations leading to huge computational efforts (see, e.g., Bauer, Reuss, & Singer, 2012, Feng, Gan, & Zhang, 2022). Our results provide the groundwork for these computations as well as for risk management, efficient calibration, hedging and optimal control of GMDBs. Further, applications in different disciplines, where randomness in space and time is also relevant, might be promising.

Related work on regime switching jump diffusion models appears in Finance on the valuation of (exotic) financial options with a fixed payment date. Numerical valuation is typically based on Laplace or Fourier inversion algorithms (see, e.g., Hieber, 2014, Hieber, 2018, Ballotta, Deelstra, & Rayée, 2017, Dong, Lv, & Wu, 2019, Le Courtois, Quittard-Pinon, & Su, 2020) or Monte-Carlo schemes like the Brownian bridge algorithm (see, e.g., Hieber & Scherer, 2010). In this strand of literature, the second part of this article is closest to Deelstra et al. (2020) that adopts the randomization technique described earlier. While this approach requires a lot of computational effort for high values of the Erlangization parameter N, we, in this article, exploit that payment dates are per se random. Small values of N are then sufficient, speeding up computations significantly.

The article is organized as follows: In Sections 2 and 3, we introduce the model framework and the payoff of GMDBs. In Section 4, we discuss how the distribution of remaining lifetime can be calibrated to a series of Erlang distributions, respectively a Laguerre series expansion. Sections 5 and 6 are the core of the paper. In Section 5, we obtain the distribution of the return at a random time $\tau_{N,\mu}$ in terms of a (closed-form) Laurent series expansion, which is useful to derive any quantiles or moments of the return. As an example, we derive valuation methods for European-type GMDBs in our regime-switching model. In Section 6, we study some path-dependent GMDBs, namely digital and lookback GMDBs. In Section 7, we demonstrate how these results apply to dynamic fund protection and dynamic withdrawal benefits. The obtained pricing formulae depend only on the solution to a series of Sylvester equations. In Section 8, we apply our technique to a calibrated example and compare our techniques to Fourier inversion algorithms.

Throughout, we use **bold** letters for vectors and matrices and abbreviate by $\mathbf{1}$ a vector of ones of appropriate size, by $\mathbf{0}$ a matrix of zeros of appropriate size and by $\boldsymbol{e}_j$ a vector where the i-th component is the Kronecker delta δ_{ji}. A $k \times k$ identity matrix is denoted by $\boldsymbol{I}_k$ and the transpose of a matrix by $'$. The matrix exponential of a matrix $\boldsymbol{B} \in \mathbb{C}^{k \times k}$ is defined via the power series $\exp(\boldsymbol{B}) := \sum_{n=0}^{\infty} \boldsymbol{B}^n / n!$.

2. Model framework

We study GMDBs embedded in variable annuities where the underlying risky asset prices are determined by

$$S_t = S_0 \, e^{X_t}, \tag{2}$$

with fixed initial price $S_0 \in \mathbb{R}_+$ and X a Markov-modulated Brownian motion (MMBM) with two-sided phase-type jumps and $X_0 = 0$. An MMBM with two-sided phase-type jumps is a stochastic process that appears in different "states" modulated by a Markov process φ_t. The main properties of the process are the following (see, e.g., Deelstra et al., 2020):

- The process $\varphi = \{\varphi_t\}_{t\ge 0}$ governs the diffusion states of the process X. It is defined on a finite state space with $M \in \mathbb{N}$ phases, that is at any time $t > 0$, $\varphi_t = j$, where $j \in \mathcal{S}_\sigma := \{1, 2, \dots, M\}$. When $\varphi_t = j$, the level X evolves like a Brownian motion with drift $d_j \in \mathbb{R}$ and variance $\sigma_j^2 > 0$. We assume that the process X_t starts in a diffusion state and that φ_0 has initial distribution $\boldsymbol{\pi} \in \mathbb{R}^{M\times 1}$.
- When $\varphi_t = j \in \mathcal{S}_\sigma$, two kinds of transitions are possible: instantaneous transitions from j to a different diffusion state $\nu \in \mathcal{S}_\sigma$ at a rate $\{\boldsymbol{Q}\}_{j\nu}$, or jumps. The rates $\{\boldsymbol{Q}\}_{j\nu}$ are collected in the subgenerator matrix[1] $\boldsymbol{Q}$. Jumps can be positive or negative; we group the different jumps in two state spaces $\mathcal{S}_+ = \{s_1^+, s_2^+, \dots, s_n^+\}$ and $\mathcal{S}_- = \{s_1^-, s_2^-, \dots, s_m^-\}$ for $n, m \in \mathbb{N}$.
- We write the dynamics of $\{X_t\}_{t\ge 0}$ as:

$$X_t = X_0 + \int_0^t d_{\varphi_s}\mathrm{d}s + \int_0^t \sigma_{\varphi_s}\mathrm{d}B_s + \int_0^t J^+_{\varphi_s}\mathrm{d}N_s^{\varphi_s,+} - \int_0^t J^-_{\varphi_s}\mathrm{d}N_s^{\varphi_s,-} . \tag{3}$$

In the diffusion state $j \in \mathcal{S}_\sigma$, the processes $\{N_t^{j,+}\}_{t\ge 0}$ and $\{N_t^{j,-}\}_{t\ge 0}$ define the arrival of jumps. More specifically, the arrival rate of an upward jump $k \in \mathcal{S}_+$ (respectively $k \in \mathcal{S}_-$ for a downward jump) is the constant $\{\boldsymbol{W}_{\sigma+}\}_{jk}$ (respectively $\{\boldsymbol{W}_{\sigma-}\}_{jk}$). The jumps may be accompanied by a change in diffusion state. If a jump $k \in \mathcal{S}_+$ appears, $\{\boldsymbol{V}_{+\sigma}\}_{ki}$ is the rate at which the jump terminates and the process returns to the diffusion state $i \in \mathcal{S}_\sigma$ (analogous the rate is $\{\boldsymbol{V}_{-\sigma}\}_{ki}$ after a downward jump $k \in \mathcal{S}_-$). If J_j^+ and J_j^- represent the absolute size of an upward and downward jump that occurred in phase j, then for all $i \in \mathcal{S}_\sigma$ and $x \ge 0$,

$$\mathbb{P}\Big(J_j^+ \in \mathrm{d}x, \varphi = i \text{ after the jump}\Big) = \frac{1}{(\boldsymbol{W}_{\sigma+}\boldsymbol{1})_j}\Big(\boldsymbol{W}_{\sigma+}e^{\boldsymbol{R}_+x}\boldsymbol{V}_{+\sigma}\Big)_{ji}\mathrm{d}x\,, \tag{4}$$

$$\mathbb{P}\Big(J_j^- \in \mathrm{d}x, \varphi = i \text{ after the jump}\Big) = \frac{1}{(\boldsymbol{W}_{\sigma-}\boldsymbol{1})_j}\Big(\boldsymbol{W}_{\sigma-}e^{\boldsymbol{R}_-x}\boldsymbol{V}_{-\sigma}\Big)_{ji}\mathrm{d}x\,. \tag{5}$$

The upward jumps have phase-type distribution represented by a subgenerator matrix $\boldsymbol{R}_+ \in \mathbb{R}^{n\times n}$ on the state space $\mathcal{S}_+$, and the downward jumps have phase-type distribution represented by a subgenerator matrix $\boldsymbol{R}_- \in \mathbb{R}^{m\times m}$ on the state space $\mathcal{S}_-$.
- For later use, we also define the transition matrices $\boldsymbol{W} \in \mathbb{R}^{M\times(n+m)}$ and $\boldsymbol{V} \in \mathbb{R}^{(n+m)\times M}$:

$$\boldsymbol{W} = \begin{bmatrix}\boldsymbol{W}_{\sigma+} & \boldsymbol{W}_{\sigma-}\end{bmatrix}, \qquad \boldsymbol{V} = \begin{bmatrix}\boldsymbol{V}_{+\sigma}\\ \boldsymbol{V}_{-\sigma}\end{bmatrix}.$$

The process does not contain an absorbing state, that is the diagonal entries of $\boldsymbol{Q}$ are determined such that $[\boldsymbol{Q}\ \boldsymbol{W}]\boldsymbol{1} = \boldsymbol{0}$.

In other words, (X, φ) can be seen as a Markov-modulated Brownian motion with two-sided phase-type jumps, in which the jumps can (but are not forced to) trigger a phase transition. When $\varphi = j \in \mathcal{S}_\sigma$, the continuous part of X is a Brownian motion with drift d_j and variance σ_j^2. In phase j, an upward jump occurs at rate $(\boldsymbol{W}_{\sigma+}\boldsymbol{1})_j$ and a downward jump occurs at rate $(\boldsymbol{W}_{\sigma-}\boldsymbol{1})_j$. Given the vector of constants $\boldsymbol{\theta} := (\theta^{(1)}, \theta^{(2)}, \dots, \theta^{(M)}) \in \mathbb{R}^M$, we introduce the process

$$\theta_t = \sum_{j\in\mathcal{S}_\sigma} \theta^{(j)} \cdot \mathbb{1}_{\varphi_t = j} = \theta^{(\varphi_t)}\,, \qquad \text{where } \varphi_t \in \mathcal{S}_\sigma\,.$$

that is constant in each phase φ_t. Finally, we define $\boldsymbol{\Theta} = \mathrm{diag}(\theta^{(j)})_{j\in\mathcal{S}_\sigma}$, the drift $\boldsymbol{D} = \mathrm{diag}(d_j)_{j\in\mathcal{S}_\sigma}$ and volatility matrix $\boldsymbol{\Sigma} = \mathrm{diag}(\sigma_j)_{j\in\mathcal{S}_\sigma}$.

Let us present the regime switching Kou model as Example 2.1. This allows a later comparison to Siu et al. (2015).

Example 2.1 (Regime switching Kou model)**.** In Kou's model, in state $j \in \mathcal{S}_\sigma$, the MMBM process X has dynamics

$$\mathrm{d}X_t = d_j\mathrm{d}t + \sigma_j\mathrm{d}W_t + \mathrm{d}J_t^{(j)}\,, \tag{6}$$

where $\{W_t\}_{t\ge 0}$ denotes a standard Brownian motion and $\{J_t^{(j)}\}_{t\ge 0}$ is an independent compound Poisson process with a constant arrival rate $\lambda_j \ge 0$ and random double-exponential jump sizes

$$\nu_j(\mathrm{d}y) = \Big(p_j\alpha_{-,j}e^{\alpha_{-,j}y}\mathbb{1}_{y<0} + (1-p_j)\alpha_{+,j}e^{-\alpha_{+,j}y}\mathbb{1}_{y\ge 0}\Big)\,\mathrm{d}y\,,$$

where with probability $p_j \in [0, 1]$, jumps are negative. Positive and negative jump sizes are exponentially distributed with intensity $\alpha_{+,j} > 0$ and $\alpha_{-,j} > 0$, respectively, see also Siu et al. (2015) for a more detailed introduction. In our notation, the regime switching Kou model is obtained as $\boldsymbol{V}_{+\sigma} = -\boldsymbol{R}_+ = \mathrm{diag}(\alpha_{+,j})_{j\in\mathcal{S}_\sigma}$, $\boldsymbol{V}_{-\sigma} = -\boldsymbol{R}_- = \mathrm{diag}(\alpha_{-,j})_{j\in\mathcal{S}_\sigma}$, $\boldsymbol{W}_{\sigma-} = \mathrm{diag}(p_j\lambda_j)_{j\in\mathcal{S}_\sigma}$, $\boldsymbol{W}_{\sigma+} = \mathrm{diag}((1-p_j)\lambda_j)_{j\in\mathcal{S}_\sigma}$ and $\boldsymbol{Q} = \boldsymbol{Q}_0 - \mathrm{diag}(\boldsymbol{W}\boldsymbol{1}) = \boldsymbol{Q}_0 - \mathrm{diag}(\lambda_j)_{j\in\mathcal{S}_\sigma}$. Given the matrix $\boldsymbol{Q}$ introduced earlier, the matrix $\boldsymbol{Q}_0 := \boldsymbol{Q} + \mathrm{diag}(\boldsymbol{W}\boldsymbol{1})$ is a generator matrix.

For later use, we recall properties of generator matrices, see Lemma 2.2.

Lemma 2.2 (Generator matrices)**.**

(a) *Let $\boldsymbol{Q}_0$ be a generator matrix of size $M \times M$ and $\boldsymbol{\Theta}$ be a diagonal matrix with real-valued entries $(\theta^{(j)})_{j\in\mathcal{S}_\sigma}$. If $\theta^{(j)} > 0$ for $j \in \mathcal{S}_\sigma$, then $\boldsymbol{Q}_0 - \boldsymbol{\Theta}$ is invertible. Furthermore, every eigenvalue of $\boldsymbol{Q}_0$ is nonpositive.*

(b) *Let $\beta > 0$ and $\boldsymbol{Q} \in \mathbb{R}^{M\times M}$ be a matrix whose eigenvalues have nonpositive real part. Then, $\beta\boldsymbol{I}_M - \boldsymbol{Q}$ is invertible and*

$$\int_0^\infty e^{-\beta t}\exp(\boldsymbol{Q}t)\mathrm{d}t = (\beta\boldsymbol{I}_M - \boldsymbol{Q})^{-1}\,.$$

Proof. See, for example, Mijatović & Pistorius (2011), Asmussen (2003), p. 55ff. □

3. GMDB payoff and discounted Laplace transform

We consider death-linked variable annuities whose benefits depend on the individual's remaining lifetime T_x. As an analoguous application, one might consider a non-life insurance contract with payments that occur at a random event time T_x. We assume that the event time T_x is independent from the financial market, i.e. the risky asset S and the Markov chain φ. More details on the distribution of T_x are given in Section 4. We are interested in evaluating quantities of the form

$$\mathbb{E}\Big[e^{-\int_0^{T_x}\theta^{(\varphi_s)}\mathrm{d}s}b(S_{T_x}, T_x, M_{T_x}, m_{T_x})\Big]\,, \tag{7}$$

where b is a payoff function and the running minimum and maximum of the process X_t is defined as

$$M_t := \sup_{s\in[0,t]} X_s\,, \quad m_t := \inf_{s\in[0,t]} X_s\,, \tag{8}$$

[1] Subgenerator matrices have non-negative off-diagonal entries; rows sum up to non-positive values. For a generator matrix, rows sum up to zero.

respectively. If $\theta^{(\varphi_s)}$, for $s \geq 0$, is the (regime-dependent) risk-free rate, this corresponds to the valuation of, for example, European, digital and lookback options under a given risk-neutral measure.[2] To derive (7), define, for $\beta \in \mathbb{R}$, the discounted Laplace transform of the process X as:

$$\phi_t^{(j)}(\beta) := \mathbb{E}\left[e^{-\int_0^t \theta^{(\varphi_s)}\,\mathrm{d}s} e^{\beta X_t} \,\middle|\, \varphi_0 = j\right]. \tag{9}$$

Lemma 3.1 states the discounted Laplace transform (9) for the Markov-modulated Brownian motion with two-sided phase-type jumps under some general existence condition. A proof of this result is, for completeness, included in Appendix A.

Lemma 3.1 (Discounted Laplace transform: Markov-modulated Brownian motion with two-sided phase-type jumps)**.** *Set $\varphi_0 = j \in \mathcal{S}_\sigma$. Let λ_0^+ be the largest eigenvalue of the subgenerator matrix $\boldsymbol{R}_+$, that is $\lambda_0^+ := \max\{\lambda : \lambda \text{ eigenvalue of } \boldsymbol{R}_+\}$. For $\beta < -\lambda_0^+$, the matrix discounted Laplace transform (9) is given by*

$$\phi_t^{(j)}(\beta) = \boldsymbol{e}_j' \exp\left(\boldsymbol{\Psi}(\beta, \boldsymbol{\Theta})t\right) \boldsymbol{1}, \tag{10}$$

with Laplace exponent matrix:

$$\begin{aligned}\boldsymbol{\Psi}(\beta, \boldsymbol{\Theta}) &= \boldsymbol{Q} + \boldsymbol{D}\beta - \boldsymbol{\Theta} + \frac{1}{2}\boldsymbol{\Sigma}^2\beta^2 + \boldsymbol{W}_{\sigma-}(\beta \boldsymbol{I}_m - \boldsymbol{R}_-)^{-1}\boldsymbol{V}_{-\sigma} \\ &\quad - \boldsymbol{W}_{\sigma+}(\beta \boldsymbol{I}_n + \boldsymbol{R}_+)^{-1}\boldsymbol{V}_{+\sigma}\,. \end{aligned} \tag{11}$$

Proof. See Appendix A. □

If the valuation is done with respect to a risk-neutral measure, the process $\{e^{-\int_0^t \theta^{(\varphi_s)}\mathrm{d}s} S_t\}_{t\geq 0}$ is a martingale. This requires a martingale condition on the parameters, see Lemma 3.2.

Lemma 3.2 (Martingale condition)**.** *If the model parameters satisfy the relation*

$$\boldsymbol{\Psi}(1, \boldsymbol{\Theta})\,\boldsymbol{1} = \boldsymbol{0}\,, \tag{12}$$

where $\boldsymbol{\Psi}(\beta, \boldsymbol{\Theta})$ is as in (11) with $\boldsymbol{\Theta} = \mathrm{diag}(\theta^{(j)})_{j\in\mathcal{S}_\sigma}$, then the process $\{e^{-\int_0^t \theta^{(\varphi_s)}\mathrm{d}s} S_t\}_{t\geq 0}$ is a martingale, that is

$$\mathbb{E}\left[e^{-\int_0^t \theta^{(\varphi_s)}\,\mathrm{d}s} S_t \,\middle|\, \varphi_0 = j\right] = S_0.$$

Proof. Note that $\phi_0^{(j)}(1) = S_0$ and

$$\left.\frac{\partial \phi_t^{(j)}(1)}{\partial t}\right|_{t=0} = \boldsymbol{e}_j' \boldsymbol{\Psi}(1, \boldsymbol{\Theta}) \cdot \exp\left(\boldsymbol{\Psi}(1, \boldsymbol{\Theta})t\right)\boldsymbol{1}\Big|_{t=0} \overset{!}{=} 0$$

is true for each j if and only if $\boldsymbol{\Psi}(1, \boldsymbol{\Theta})\,\boldsymbol{1} = \boldsymbol{0}$. See also Deelstra et al. (2020). □

Let us first continue Example 2.1, see Example 3.3.

Example 3.3 (Regime switching Kou model (continued))**.** Given the Laplace exponent matrix

$$\begin{aligned}\boldsymbol{\Psi}(\beta, \boldsymbol{\Theta}) &= \boldsymbol{Q} + \boldsymbol{D}\beta - \boldsymbol{\Theta} + \frac{1}{2}\boldsymbol{\Sigma}^2\beta^2 + \boldsymbol{W}_{\sigma-}(\beta \boldsymbol{I}_M - \boldsymbol{R}_-)^{-1}\boldsymbol{V}_{-\sigma} \\ &\quad - \boldsymbol{W}_{\sigma+}(\beta \boldsymbol{I}_M + \boldsymbol{R}_+)^{-1}\boldsymbol{V}_{+\sigma} \\ &= \boldsymbol{Q}_0 + \boldsymbol{D}\beta - \boldsymbol{\Theta} + \frac{1}{2}\boldsymbol{\Sigma}^2\beta^2 \\ &\quad + \mathrm{diag}\left(\lambda_j p_j \frac{\alpha_{-,j}}{\alpha_{-,j} + \beta} + \lambda_j(1 - p_j)\frac{\alpha_{+,j}}{\alpha_{+,j} - \beta} - \lambda_j\right), \end{aligned}$$

the martingale condition $\boldsymbol{\Psi}(1, \boldsymbol{\Theta})\,\boldsymbol{1} = \boldsymbol{0}$ is simplified to:

$$d_j = \theta^{(j)} - \frac{1}{2}\sigma_j^2 - \left(\lambda_j p_j \frac{\alpha_{-,j}}{\alpha_{-,j}+1} + \lambda_j(1 - p_j)\frac{\alpha_{+,j}}{\alpha_{+,j}-1} - \lambda_j\right) \tag{13}$$

for $j \in \mathcal{S}_\sigma$. In each phase $j \in \mathcal{S}_\sigma$, this is the Black-Scholes drift minus the correction for jumps. In case of Kou's model ($M = 1$), the Laplace exponent is given by:

$$\begin{aligned}\boldsymbol{\Psi}(\beta, \boldsymbol{\Theta}) &= d_1\beta - \theta^{(1)} + \frac{1}{2}{\sigma_1}^2\beta^2 \\ &\quad + \lambda_1\left(p_1 \frac{\alpha_{-,1}}{\alpha_{-,1} + \beta} + (1 - p_1)\frac{\alpha_{+,1}}{\alpha_{+,1} - \beta} - 1\right). \end{aligned} \tag{14}$$

We consider a second example where the downward jump distribution approximates heavier, power-type tails, see Example 3.4.

Example 3.4 (Phase-type jump model)**.** See also Robert & Boudec (1997) and Deelstra et al. (2020) for a more detailed analysis and motivation. We consider two diffusion phases ($M = 2$). The transition from phase 1 to phase 2 is defined by a more general phase-type distribution with subgenerator matrix:

$$\boldsymbol{R}_- = \begin{bmatrix} -(c + s_a) & 1/a & (1/a)^2 & \cdots & (1/a)^{n_a-1} \\ b/a & -b/a & 0 & \cdots & 0 \\ (b/a)^2 & 0 & -(b/a)^2 & \cdots & 0 \\ \vdots & & & & 0 \\ (b/a)^{n_a-1} & 0 & 0 & \cdots & -(b/a)^{n_a-1} \end{bmatrix}$$

with $n_a \in \mathbb{N}$, $a > \max(1, b)$, $b, c > 0$ and $s_a = 1/a + 1/a^2 + \ldots + 1/a^{n_a-1}$. The other matrices are chosen as follows for parameters $\lambda > 0$, $q_1 > 0$, $q_2 > 0$, $\boldsymbol{R}_+ = -\lambda$, $\varphi_0 = 1$, $\boldsymbol{V}_{+\sigma} = \begin{bmatrix}\lambda & 0\end{bmatrix}$:

$$\boldsymbol{Q} = \begin{bmatrix} -q_1 & 0 \\ 0 & -q_2 \end{bmatrix}, \quad \boldsymbol{W}_{\sigma-} = \begin{bmatrix} q_1 & 0 & \cdots & 0 \\ 0 & 0 & \cdots & 0 \end{bmatrix},$$

$$\boldsymbol{W}_{\sigma+} = \begin{bmatrix} 0 \\ q_2 \end{bmatrix}, \quad \boldsymbol{V}_{-\sigma} = \begin{bmatrix}\boldsymbol{0} & -\boldsymbol{R}_-\boldsymbol{1}\end{bmatrix}.$$

Phase-type distributions can only approximate heavy-tailed distributions. However, as Fig. 1 demonstrates, these approximations can be pretty reasonable in practical applications. In the figure, the quantiles of a Pareto distribution with density $f(x) = \alpha x_m^\alpha / x^{\alpha+1}\mathbb{1}_{x\geq x_m}$, $\alpha > 1$, are compared to three phase-type approximations with parameters (a, b, c, n_a) and the distribution $|X|$, where $X \sim \mathcal{N}(0, 1)$. The means of the distribution are chosen to be equal to $\mathbb{E}[|X|] = \sqrt{2/\pi} = \alpha x_m/(\alpha - 1) = \frac{1}{c}\sum_{l=0}^{n_a-1}\left(\frac{1}{b}\right)^l$, see also Deelstra et al. (2020).

4. Distribution of remaining lifetime: approximation by Erlang random variable

Having discussed the dynamics of the underlying risky asset prices, this section deals with the random payment date T_x. As mentioned in the introduction, it turns out that calculations are surprisingly simple for an exponential or Erlang time $\tau_{N,\mu}$. In this section, we show how any distribution of the payment date T_x can well be approximated by combinations of Erlang random variables. This has theoretical foundation in the link to a Laguerre series expansion discussed in Section 4.2, see also Zhang & Yong (2019). In the following, denote by f_{T_x} the density of the remaining lifetime T_x.

4.1. Approximation by a combination of Erlang densities

We assume that the density function of the remaining lifetime T_x can be approximated by a combination of Erlang densities:

$$f_{T_x}(t) \approx \sum_{k=0}^{K_B} B_k \cdot f_{\tau_{n_k,\mu_k}}(t) =: \hat{f}_{T_x}(t)\,, \tag{15}$$

[2] Note that the risk neutral measure associated to a regime switching model is not unique in general. When starting from the real-world probability measure, one of the most common approaches is to use the regime switching random Esscher transform to determine a risk neutral measure. This transform has the advantages of preserving the (Markov-modulated) nature of the model and of minimising the conditional relative entropy with respect to the historical measure (see e.g. Elliott, Chan, & Siu, 2005 for details and Godin & Trottier, 2019 for a recent discussion).

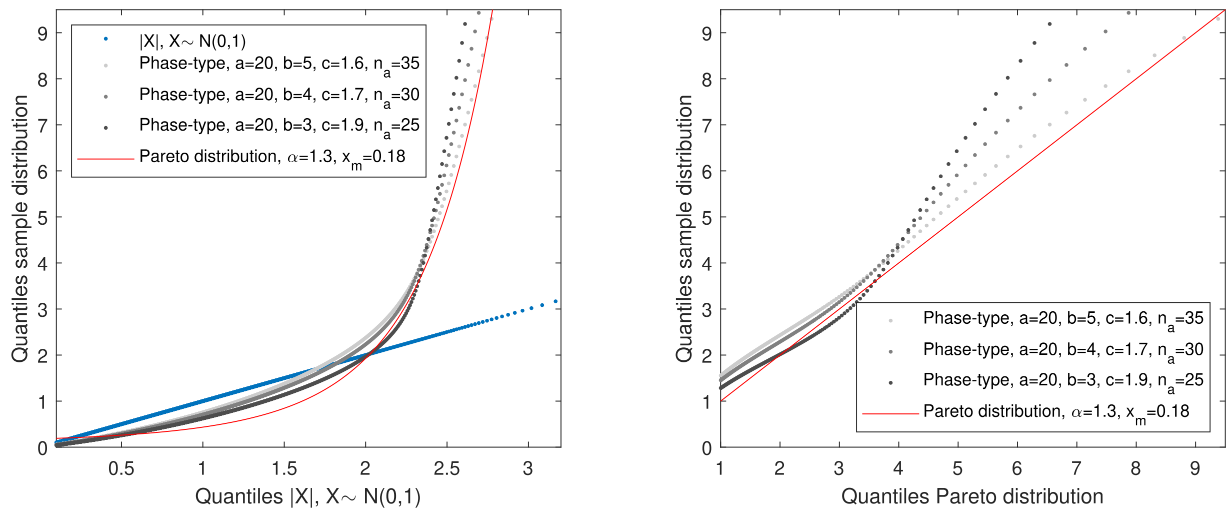

Fig. 1. QQ-Plot comparing the quantiles of a Pareto($\alpha = 1.3$, $x_M = 0.18$) distribution to the distribution of the absolute value of a standard normal distribution and different phase-type approximations.

for constants $K_B \in \mathbb{N}$, $B_k \in \mathbb{R}$ with $\sum_{k=0}^{K_B} B_k = 1$. A major property of (finite) mixtures of Erlang distributions is the fact that they can arbitrarily well approximate any distribution on $[0, \infty)$, see, e.g., p. 84 in Asmussen (2003). Exploiting that the remaining lifetime T_x is independent of the risky asset, we can reduce the previously introduced valuation problems to the valuation problem relative to an Erlang distributed remaining lifetime. Exemplarily, in the case of a European-type payoff $b(S_{T_x})$, this means that:

$$\begin{aligned}\mathbb{E}\left[e^{-\int_0^{T_x}\theta(\varphi_s)\,\mathrm{d}s} b(S_{T_x})\right] &\approx \sum_{k=0}^{K_B} B_k \int_0^\infty \mathbb{E}\left[e^{-\int_0^{t}\theta(\varphi_s)\,\mathrm{d}s} b(S_t)\right] f_{\tau_{n_k,\mu_k}}(t)\,\mathrm{d}t \\ &= \sum_{k=0}^{K_B} B_k \cdot \mathbb{E}\left[e^{-\int_0^{\tau_{n_k,\mu_k}}\theta(\varphi_s)\,\mathrm{d}s} b\left(S_{\tau_{n_k,\mu_k}}\right)\right],\end{aligned}$$

for $n_k \in \mathbb{N}$ and $\mu_k > 0$. The special case of exponential random variables ($n_k = 1$) is discussed and calibrated to a life table by Siu et al. (2015).

4.2. Approximation by Laguerre series expansion

Laguerre functions are defined as

$$\begin{aligned}\Psi_N(t) &= \sqrt{2\mu}\, e^{-\mu t} \cdot \sum_{k=0}^{N} (-1)^k \binom{N}{k} \frac{(2\mu t)^k}{k!} \\ &= \sum_{k=0}^{N} (-2)^k \sqrt{\frac{2}{\mu}} \binom{N}{k} \cdot f_{\tau_{k+1,\mu}}(t),\end{aligned}$$

for $N = 1, 2, \dots$ and $t > 0$ and form a complete orthonormal basis of square integrable functions on the positive real line. We can expand the density $f_{T_x} \in L^2(\mathbb{R}_+)$ as:

$$f_{T_x}(t) = \sum_{k=0}^{\infty} A_k \cdot \Psi_k(t) \approx \sum_{k=0}^{K_A} A_k \cdot \Psi_k(t) =: \tilde{f}_{T_x}(t). \tag{16}$$

It is easy to show that this approximation by Laguerre series is a special case of (15), see also Zhang & Yong (2019) for a more detailed discussion. The advantage of the Laguerre series expansion is that it allows for an error analysis of the truncation error, see the more detailed discussion in Section 8. In the following, we focus on the case where the remaining lifetime T_x is an Erlang distributed random variable $\tau_{N,\mu}$.

5. European-type GMDBs and Laurent series expansion

Now, we consider European-type GMDBs. At time $T_x = \tau_{N,\mu}$, the payoff is a function b of the risky asset price S_{T_x}. The time-0 value of this product is

$$P_V(S_0) = \mathbb{E}\left[e^{-\int_0^{\tau_{N,\mu}}\theta(\varphi_s)\,\mathrm{d}s} b\left(S_{\tau_{N,\mu}}\right)\right]. \tag{17}$$

An example is a simple guarantee product with guarantee level $K \geq 0$, that is $b(S_{\tau_{N,\mu}}) = \max(S_{\tau_{N,\mu}} - K, 0)$. We want to first obtain the density of $X_{\tau_{N,\mu}} = \ln(S_{\tau_{N,\mu}}/S_0)$, the logarithmic return until a (random) Erlang time $\tau_{N,\mu}$, independent of X.

The discounted Laplace transform of the subordinated process $X_{\tau_{N,\mu}}$ is known, see Lemma 5.1. To keep the paper self-contained, we provide a short proof in the Appendix.

Lemma 5.1 (Laplace transform of Erlang-subordinated process)**.** *Consider an Erlang random variable (r.v.) $\tau_{N,\mu}$. Assume that $\beta \leq -\lambda_0^+$ where $\lambda_0^+ := \max\{\lambda : \lambda$ eigenvalue of $\boldsymbol{R}_+\}$. Further assume that the eigenvalues of $\boldsymbol{\Psi}(\beta, \boldsymbol{\Theta})$ have nonpositive real part only.*[3] *For $j \in \mathcal{S}_\sigma$:*

$$\begin{aligned}\phi^{(j)}_{\tau_{N,\mu}}(\beta) &= \mathbb{E}\left[e^{-\int_0^{\tau_{N,\mu}}\theta(\varphi_s)\,\mathrm{d}s + \beta X_{\tau_{N,\mu}}} \,\middle|\, \varphi_0 = j\right] \\ &= \boldsymbol{e}'_j \left(\mu^N (\mu \boldsymbol{I}_M - \boldsymbol{\Psi}(\beta, \boldsymbol{\Theta}))^{-N}\right) \boldsymbol{1}.\end{aligned} \tag{18}$$

Proof. See Appendix B. □

Without regime switching ($M = 1$), (18) simplifies to

$$\phi^{(1)}_{\tau_{N,\mu}}(\beta) = \left(\frac{\mu}{\mu - \boldsymbol{\Psi}(\beta, \boldsymbol{\Theta})}\right)^N, \tag{19}$$

see, for example, Gerber, Shiu, & Yang (2013). In the general case of $M \geq 1$, we expand $\phi^{(j)}_{\tau_{N,\mu}}(\beta)$ as a Laurent series, see Lemma 5.2.

Lemma 5.2 (Laurent series expansion of $\phi^{(j)}_{\tau_{N,\mu}}(\beta)$)**.**

(a) *The Laplace transform*

$$\phi^{(j)}_{\tau_{N,\mu}}(\beta) = \boldsymbol{e}'_j \left(\mu^N (\mu \boldsymbol{I}_M - \boldsymbol{\Psi}(\beta, \boldsymbol{\Theta}))^{-N}\right) \boldsymbol{1}$$

[3] This assumption is not restrictive as it is usually satisfied for reasonable parameter choices. In specific examples, it is possible to derive conditions that are easier to check, Siu et al. (2015) propose for example $\mu + r > \min_{j \in \mathcal{S}_\sigma} \kappa_j(\beta)$, where $\kappa_j(\beta)$ is introduced in our Example 5.4, Eq. (25).

can be written as the quotient $p(\beta)/q(\beta)$ of two polynomials $p(\beta)$ and $q(\beta)$, where we assume (without loss of generality) that $p(\beta)$ and $q(\beta)$ have no common roots.

(b) *Denote by $\{\alpha_i\}$ and $\{\beta_k\}$ the roots of the polynomial $q(\beta)$ in (a) with negative and positive real part, respectively.*[4] *We can expand $\phi^{(j)}_{\tau_{N,\mu}}(\beta)$ in terms of its Laurent series:*

$$\phi^{(j)}_{\tau_{N,\mu}}(\beta) = \sum_i \sum_{z=1}^{N} \frac{a_{iz}}{(\alpha_i-\beta)^z} + \sum_k \sum_{z=1}^{N} \frac{b_{kz}}{(\beta_k-\beta)^z}\,. \tag{20}$$

The coefficients a_{iz}, b_{kz} are uniquely determined solving:

$$a_{iz} = \frac{(-1)^z}{(N-z)!} \lim_{\beta\to\alpha_i} \frac{\mathrm{d}^{N-z}}{\mathrm{d}\beta^{N-z}} \Big((\beta-\alpha_i)^N \cdot \phi^{(j)}_{\tau_{N,\mu}}(\beta) \Big), \tag{21}$$

$$b_{kz} = \frac{(-1)^z}{(N-z)!} \lim_{\beta\to\beta_k} \frac{\mathrm{d}^{N-z}}{\mathrm{d}\beta^{N-z}} \Big((\beta-\beta_k)^N \cdot \phi^{(j)}_{\tau_{N,\mu}}(\beta) \Big). \tag{22}$$

Proof.

(a) As the matrix inverse $\boldsymbol{A}^{-1}$ can be expressed in terms of the determinants and the subdeterminants of $\boldsymbol{A}$, the entries of the matrices $(\beta\boldsymbol{I}_n+\boldsymbol{R}_+)^{-1}$ and $(-\beta\boldsymbol{I}_m+\boldsymbol{R}_-)^{-1}$ are (quotients of) polynomials, see Asmussen (2003), p. 83. The same arguments show that $\big(\mu\boldsymbol{I}_M - \boldsymbol{\Psi}(\beta,\boldsymbol{\Theta})\big)^{-1}$ is the quotient of two polynomials.

(b) The polynomial $q(\beta)$ does not have a root with zero real part. This can be seen as follows: For each purely imaginary z, it holds that $\big|\mathbb{E}\big[e^{zX_{\tau_{N,\mu}}}\big]\big| \le \mathbb{E}\big[\big|e^{zX_{\tau_{N,\mu}}}\big|\big] = \mathbb{E}[1] = 1$ (see Gerber et al., 2013, p. 617). If $p(\beta)$ and $q(\beta)$ have no common roots, q has simple roots and the degree of q is greater than the degree of p, it is possible to form a partial fraction decomposition with Laurent series (21) and (22), see, e.g., (1) in Eustice & Klamkin (1979).

□

If at least one of the $\theta^{(j)}$s in the diagonal matrix $\boldsymbol{\Theta}$ is positive, the Markov chain φ is absorbing. If the Markov chain is absorbed at time t, we denote its state by $\varphi_s = \star$ for all $s \ge t$. Given one realization of the time $\tau_{N,\mu}$ and the evolution of the Markov chain until that time, the probability that the chain has not moved to the absorbing state is $e^{-\int_0^{\tau_{N,\mu}} \theta(\varphi_s)\,\mathrm{d}s}$. With the results in Lemma 5.2, we can apply the residue theorem and obtain the density of $X_{\tau_{N,\mu}}$ given the initial state $\varphi_0 = j$. If $\boldsymbol{\Theta} = \boldsymbol{0}$, this density is a sum of Erlang densities:

$$f_{X_{\tau_{N,\mu}}}(x) = \begin{cases} \sum_i \sum_{z=1}^{N} (-a_{iz}) \frac{x^{z-1}}{(z-1)!} e^{-\alpha_i x}, & x < 0 \\ \sum_k \sum_{z=1}^{N} b_{kz} \frac{x^{z-1}}{(z-1)!} e^{-\beta_k x}, & x \ge 0 \end{cases} \tag{23}$$

Given the density (23), it is not only possible to estimate GMDB values but also related risk measures like Value-at-Risk (VaR) and Conditional-Tail-Expectation (CTE). If $\boldsymbol{\Theta} \ne \boldsymbol{0}$, i.e. if at least one of the $\theta^{(j)}$s is positive, the Markov chain is absorbing and the absorption probability is given by $\mathbb{P}\big(\varphi_{\tau_{N,\mu}} = \star\big) = 1 - \int_{\mathbb{R}} f_{X_{\tau_{N,\mu}}}(x)\,\mathrm{d}x$ with $f_{X_{\tau_{N,\mu}}}(x)$ as in (23). In this case, the density of $X_{\tau_{N,\mu}}$ is composed of a point mass at the absorbing state $\varphi_{\tau_{N,\mu}} = \star$ and the (defective) density (23) of the "survived" paths. This concept of a (defective) density allows to extend the discounted density approach by Gerber et al. (2012, 2013) to regime switching models. To link to this research and for illustrative purposes, Example 5.3 presents the coefficients in (23) in the Black-Scholes model.

Example 5.3 (Black-Scholes model)**.** In a Black-Scholes model with $d_1 = r - \sigma^2/2$, the discounted Laplace transform is given by (19). The (non-removable) singularities are then given by the roots of the equation $\boldsymbol{\Psi}(\beta,\boldsymbol{\Theta}) = \mu$, i.e.

$$\boldsymbol{\Psi}(\beta,\boldsymbol{\Theta}) - \mu = \frac{1}{2}\sigma^2\beta^2 + \Big(r - \frac{1}{2}\sigma^2\Big)\beta - \theta^{(1)} - \mu = 0\,, \tag{24}$$

an equation that can be solved to

$$\alpha_1 = \frac{1}{2} - \frac{r}{\sigma^2} - \sqrt{\Big(\frac{r}{\sigma^2} - \frac{1}{2}\Big)^2 + \frac{2(\mu+\theta^{(1)})}{\sigma^2}}\,,$$

$$\beta_1 = \frac{1}{2} - \frac{r}{\sigma^2} + \sqrt{\Big(\frac{r}{\sigma^2} - \frac{1}{2}\Big)^2 + \frac{2(\mu+\theta^{(1)})}{\sigma^2}}\,.$$

With some algebra, it is easy to show that $\alpha_1 \cdot \beta_1 = -2(\mu + \theta^{(1)})/\sigma^2$. We get for $z = 1, 2, \ldots, N$:

$$\begin{aligned} a_{1z} &= \frac{(-1)^z}{(N-z)!} \lim_{\beta\to\alpha_1} \frac{\mathrm{d}^{N-z}}{\mathrm{d}\beta^{N-z}} \left((\beta-\alpha_1)^N \frac{\mu^N}{\big(\mu - \boldsymbol{\Psi}(\beta,\boldsymbol{\Theta})\big)^N} \right) \\ &= (-1)^z \frac{(-1)^{N-z}\binom{2N-z-1}{N-1}}{(\alpha_1-\beta_1)^{N-z}} \left(\frac{\mu}{-\frac{1}{2}\sigma^2(\alpha_1-\beta_1)} \right)^N \\ &= (-1)^z \frac{\binom{2N-z-1}{N-1}}{(\beta_1-\alpha_1)^{N-z}} \left(\frac{-\alpha_1\beta_1}{\beta_1-\alpha_1} \right)^N \cdot \left(\frac{\mu}{\mu+\theta^{(1)}} \right)^N, \\ b_{1z} &= \frac{1}{(-1)^N} \frac{1}{(-1)^{N-z}} a_{1z} = (-1)^z a_{1z}\,. \end{aligned}$$

If $\theta^{(1)} = 0$, (23) defines a density; else the factor $(\mu/(\mu+\theta^{(1)}))^N$ makes (23) a defective density. For the density of $X_{\tau_{N,\mu}}$ in a Black-Scholes model, see (2.36) in Gerber et al. (2012).

We further demonstrate the procedure on how to obtain (23) in the example of the regime switching Kou model, studied in detail by Siu et al. (2015), see Example 5.4.

Example 5.4 (Regime switching Kou model (continued))**.** Consider again the regime switching Kou model from Example 3.3. We discuss the case of $M = 2$ regimes. The general case of M regimes in, for example, Siu et al. (2015), can be treated analoguously. Abbreviate

$$\begin{aligned} \kappa_j(\beta) :&= d_j\beta - \theta^{(j)} + \frac{1}{2}\sigma_j^2\beta^2 \\ &\quad + \lambda_j \left(p_j \frac{\alpha_{-,j}}{\alpha_{-,j}+\beta} + (1-p_j)\frac{\alpha_{+,j}}{\alpha_{+,j}-\beta} - 1 \right) \end{aligned} \tag{25}$$

for $j = 1, 2$. Note that $q_{jj} := (\boldsymbol{Q}_0)_{jj}$ is non-positive and define:

$$d(\beta) := (q_{11} + \kappa_1(\beta) - \mu)(q_{22} + \kappa_2(\beta) - \mu) - q_{11}q_{22}\,.$$

With this, the Laplace transform from Lemma 5.1 is given by:[5]

$$\begin{aligned} \phi^{(j)}_{\tau_{N,\mu}}(\beta) &= \boldsymbol{e}_j' \left(\mu^N \big(\mu\boldsymbol{I}_M - \boldsymbol{\Psi}(\beta,\boldsymbol{\Theta})\big)^{-N} \right) \boldsymbol{1} \\ &= \boldsymbol{e}_j' \left(\mu^N \left(-\boldsymbol{Q}_0 - \begin{bmatrix} \kappa_1(\beta)-\mu & 0 \\ 0 & \kappa_2(\beta)-\mu \end{bmatrix} \right)^{-N} \right) \boldsymbol{1} \\ &= \boldsymbol{e}_j' \left(\left(\mu^N \left(- \begin{bmatrix} q_{11} & -q_{11} \\ -q_{22} & q_{22} \end{bmatrix} - \begin{bmatrix} \kappa_1(\beta)-\mu & 0 \\ 0 & \kappa_2(\beta)-\mu \end{bmatrix} \right)^{-N} \right) \boldsymbol{1} \end{aligned}$$

[4] We assume these roots are simple roots. In case of equal roots, the following expansion is easily modified.

[5] Note that the inverse of a 2×2 matrix is given by:

$$A^{-1} := \begin{bmatrix} a & b \\ c & d \end{bmatrix}^{-1} = \frac{1}{\det(A)} \begin{bmatrix} d & -b \\ -c & a \end{bmatrix}.$$

$$= \boldsymbol{e}_j' \left(\left(\mu^N \left(\begin{bmatrix} -q_{11} - \kappa_1(\beta) + \mu & q_{11} \\ q_{22} & -q_{22} - \kappa_2(\beta) + \mu \end{bmatrix}^{-1} \right)^N \right) \boldsymbol{1}$$

$$= \boldsymbol{e}_j' \left(\left(\frac{\mu}{d(\beta)} \right)^N \left(\begin{bmatrix} -q_{22} - \kappa_2(\beta) + \mu & -q_{11} \\ -q_{22} & -q_{11} - \kappa_1(\beta) + \mu \end{bmatrix}^N \right) \right) \boldsymbol{1} ,$$

a function that can indeed be written as a quotient of two polynomials. For example, Siu et al. (2015) show that, given the condition $-\infty < -\alpha_{-,2} < -\alpha_{-,2} < 0 < \alpha_{+,1} < \alpha_{+,2} < \infty$, the equation $d(\beta) = 0$ has 4 solutions with positive real part $\beta_1, \beta_2, \beta_3, \beta_4$ and 4 solutions with negative real part $\alpha_1, \alpha_2, \alpha_3, \alpha_4$, ordered as $-\infty < \alpha_4 < \alpha_3 < \alpha_2 < \alpha_1 < 0 < \beta_1 < \beta_2 < \beta_3 < \beta_4 < \infty$, see Lemma A.5 in the Appendix of Siu et al. (2015). With these coefficients, the (defective) density of $X_{\tau_{N,\mu}}$ is explicitly given by (21)–(23).

Given initial state $\varphi_0 = j \in \mathcal{S}_\sigma$, (18) writes as:

$$\mathbb{E}\left[e^{-\int_0^{\tau_{N,\mu}} \theta(\varphi_s)\,\mathrm{d}s} S_{\tau_{N,\mu}} \right] = \mathbb{E}\left[S_0 e^{X_{\tau_{N,\mu}} - \int_0^{\tau_{N,\mu}} \theta(\varphi_s)\,\mathrm{d}s} \right]$$
$$= S_0\, \boldsymbol{e}_j' \left(\mu^N \left(\mu \boldsymbol{I}_M - \boldsymbol{\Psi}(1, \boldsymbol{\Theta}) \right)^{-N} \right) \boldsymbol{1} .$$

Representing the (defective) density as in (23) allows us to value European-type GMDBs in closed-form. The advantage of working with (defective) densities is the fact that the discount rate is modelled as an absorption rate of the Markov chain. With this idea, values of European-type GMDBs with payoff $b(S_t)$, paid at an Erlang random time $t = \tau_{N,\mu}$, can be written as:

$$\begin{aligned} V(\mu, r) : &= \mathbb{E}\left[e^{-\int_0^{\tau_{N,\mu}} \theta(\varphi_s)\,\mathrm{d}s} b\left(S_{\tau_{N,\mu}}\right) \right] \\ &= \mathbb{E}\left[\mathbb{E}\left[e^{-\int_0^{\tau_{N,\mu}} \theta(\varphi_s)\,\mathrm{d}s} b\left(S_0 e^{X_{\tau_{N,\mu}}}\right) \,\middle|\, \varphi,\ \tau_{N,\mu} \right] \right] \\ &= \mathbb{E}\left[\mathbb{E}\left[0 \cdot \left(1 - e^{-\int_0^{\tau_{N,\mu}} \theta(\varphi_s)\,\mathrm{d}s}\right) \right.\right. \\ &\quad \left.\left. + \int_{\mathbb{R}} b\left(S_0 e^x\right) f_{X_{\tau_{N,\mu}}}(x)\,\mathrm{d}x \,\middle|\, \varphi,\ \tau_{N,\mu} \right] \right] \\ &= \int_{\mathbb{R}} b\left(S_0 e^x\right) f_{X_{\tau_{N,\mu}}}(x)\,\mathrm{d}x , \end{aligned} \tag{26}$$

with the (defective) density $f_{X_{\tau_{N,\mu}}}(x)$ from (23). Note that with (26) we need to compute the integral with respect to the terminal payoff only – the discount factor is "integrated" into the (defective) density. Theorem 5.5 gives the final result.

Theorem 5.5 (European-type options)**.** *Consider European-type GMDBs with payoff $b(S_t)$, paid at an Erlang random time $t = \tau_{N,\mu}$. Their fair value is given by*

$$\begin{aligned} V(\mu, r) : &= \mathbb{E}\left[e^{-\int_0^{\tau_{N,\mu}} \theta(\varphi_s)\,\mathrm{d}s} b\left(S_{\tau_{N,\mu}}\right) \right] \\ &= \sum_i \sum_{z=1}^N \int_{-\infty}^0 b(S_0 e^x) \cdot (-a_{iz}) \frac{x^{z-1}}{(z-1)!} e^{-\alpha_i x}\,\mathrm{d}x \\ &\quad + \sum_k \sum_{z=1}^N \int_0^\infty b(S_0 e^x) \cdot b_{kz} \frac{x^{z-1}}{(z-1)!} e^{-\beta_k x}\,\mathrm{d}x . \end{aligned} \tag{27}$$

Proof. Simply plug (23) into (26). The case of one state $M = 1$ relates to the discounted density approach by Gerber et al. (2012, 2013). In this case, one can derive much simpler relations between the value with and without discount factor, see, e.g., (1.8) in Gerber et al. (2013) or Example 5.3 above. Note that our case of a regime-dependent discount factor leads to a dependence between discount factor and asset value $S_{\tau_{N,\mu}}$. □

Nicely, for many popular GMDBs, the integrals in (27) can be solved analytically, see also, e.g., Gerber et al. (2012, 2013), Zhang & Yong (2019) in the case of the Black-Scholes and Kou model. Let us just apply our results to an out-of-the money call GMDB, see Example 5.6.

Example 5.6 (Out-of-the-money call option valuation)**.** For $b(S_t) = \max(S_t - K, 0)$, $\Re(h) > 1$ and $S_0 \le K$, we obtain:

$$\begin{aligned} C(h, z) : &= \int_0^\infty e^{-hx} \frac{x^{z-1}}{(z-1)!} \max(S_0 e^x - K, 0)\mathrm{d}x \\ &= \int_{\ln(K/S_0)}^\infty e^{-hx} \frac{x^{z-1}}{(z-1)!} (S_0 e^x - K)\mathrm{d}x \\ &= S_0 \cdot \eta\left(\ln(K/S_0), h-1, z\right) - K \cdot \eta\left(\ln(K/S_0), h, z\right) , \end{aligned}$$

where we use that for $y \ge 0$, we can apply partial integration to obtain

$$\eta(y, h, z) = \int_y^\infty e^{-hx} \frac{x^{z-1}}{(z-1)!}\mathrm{d}x = \sum_{i=1}^z e^{-hy} \frac{1}{h^{z+1-i}} \frac{y^{i-1}}{(i-1)!} .$$

From (27), we finally obtain:

$$C(S_0) := \mathbb{E}\left[e^{-\int_0^{\tau_{N,\mu}} \theta_s \mathrm{d}s} b\left(S_{\tau_{N,\mu}}\right) \right] = \sum_k \sum_{z=1}^N b_{kz} C(\beta_k, z) , \tag{28}$$

where the coefficients b_{kz} are given by (22) and β_k are the (non-removable) singularities with positive real part of $\phi_{\tau_{N,\mu}}(\beta)$. Note that the singularities β_k and the coefficients b_{kz} depend on the discount factor via the matrix $\boldsymbol{\Theta}$.

Similarly, one can value in-the-money call GMDBs. The corresponding put options can easily be expressed using put-call parity. Note that the valuation (27) does not require any inverse Laplace transform. Instead, most common option types allow to solve the integrals in (27) analytically. As Laplace inversion techniques may be computationally expensive or require high-precision arithmetic (see, for example, Hassanzadeh & Pooladi-Darvish, 2007 for a comparison of different algorithms), this is an advantage over the pricing equations presented in, for example, Section 3.1 in Siu et al. (2015). The closed-form density (23) allows also to easily compute higher-order moments and other risk measures such as the Value-at-Risk (VaR) and the Conditional-Tail-Expectation (CTE).

6. Path-dependent GMDBs and Sylvester equations

Deelstra et al. (2020) derive by randomization and fluidization approximations for fixed-time European digital options, vanilla options and down-and-out options in a Markov-modulated Brownian motion framework with two-sided phase-type jumps. For high values of N, replacing the fixed maturity time T by a $\tau_{N,\frac{\mu}{N}}$ random variable leads to accurate approximations of the option price. We first want to point out that these results are useful in life insurance when combined with the remaining lifetime approximations presented in Section 4.

In this section, we further focus on more complex GMDB options (with maturity T_x), which may depend on the time-$\tau_{N,\mu}$ maximum $S_0 e^{M_{\tau_{N,\mu}}}$ or minimum $S_0 e^{m_{\tau_{N,\mu}}}$ of the underlying risky asset process. A lookback GMDB, for example, returns an option on the maximum of the asset value at time $\tau_{N,\mu}$. To evaluate such a lookback option in the asset model with regime switching and two-sided phase-type jumps, together with an Erlang distributed death time, we follow Deelstra et al. (2020) and combine fluidization (see, for example, Rogers, 1994, Jiang & Pistorius, 2008 or Kijima & Siu, 2014) and Erlangization techniques (see, for example, Asmussen & Albrecher, 2010, Ch. IX.8). Applications to dynamic witdrawal benefits and dynamic fund protection are discussed in Section 7. For the sake of the readability of the paper, we introduce in the following subsections all necessary notations and notions, and we include a derivation of the digital option formulae since these will be used for the evaluation of lookback options. We include several examples and links to the literature.

6.1. Fluidization and Erlangization techniques

The idea of fluidization is to replace jumps in the process X_t by additional phases with zero volatility and slope 1 (positive jumps), respectively -1 (negative jumps). We denote this approximating process by Y_t and introduce a new Markov chain $\zeta = \{\zeta_t\}_{t\ge 0}$ that for $\zeta \in \mathcal{S}_\sigma$ behaves as φ but has additional "jump states", that is $\zeta \in \mathcal{S} := \mathcal{S}_\sigma \cup \mathcal{S}_- \cup \mathcal{S}_+$. The pairs (X_t, φ_t) and (Y_t, ζ_t) relate by the random time

$$\mathcal{T}(t) = \int_0^t \mathbb{1}_{\varphi_s \in \mathcal{S}_\sigma}\, \mathrm{d}s\,,$$

that ticks whenever X_t is in one of the diffusion states $\varphi_t \in \mathcal{S}_\sigma$. As the process X_t starts in a diffusion state, the initial distribution of the Markov chain ζ_t is given by $[\boldsymbol{\pi}\, \mathbf{0}_n\, \mathbf{0}_m]$, i.e. $\zeta_0 = \varphi_0$. Time evolves until this random time $\mathcal{T}(t)$ reaches the Erlang distributed time of death $\tau_{N,\mu}$. With this construction, the distribution of X_t is equal to the distribution of $Y_{\mathcal{T}^{-1}(t)}$ for all times $t < \tau_{N,\mu}$. This also implies that the levels crossed by X on $[0, t)$ are the same as the ones crossed by Y on $[0, \mathcal{T}^{-1}(t))$ and that Markov chains in diffusion states agree: $\zeta_{\mathcal{T}^{-1}(t)} = \varphi_t$ for $t \ge 0$. The advantage of introducing the process Y is that it is a continuous process which significantly simplifies the analysis of its maximum and first-passage time.

6.1.1. Exponential time $\tau_{1,\mu}$

As in Section 5, we model an absorption at a rate $\theta^{(\zeta_s)}$ if the process Y is in a diffusion state $\zeta_s \in \mathcal{S}_\sigma$, i.e. the state space of ζ is indeed $\zeta \in \mathcal{S} \cup \star$ for an absorption state $\star$. For $\boldsymbol{\Theta} = \mathrm{diag}(\theta^{(j)})_{j\in\mathcal{S}_\sigma}$, the generator of the process Y is:

$$G = \left[\begin{array}{c|ccc} 0 & \mathbf{0} & \mathbf{0} & \mathbf{0} \\ \hline \mu \boldsymbol{I}_M & & & \\ \mathbf{0} & & \mathcal{P}(\boldsymbol{\Theta}) & \\ \mathbf{0} & & & \end{array}\right], \quad \text{where}$$

$$\mathcal{P}(\boldsymbol{\Theta}) := \begin{bmatrix} \boldsymbol{Q} - \mu \boldsymbol{I}_M - \boldsymbol{\Theta} & \boldsymbol{W}_{\sigma+} & \boldsymbol{W}_{\sigma-} \\ \boldsymbol{V}_{+\sigma} & \boldsymbol{R}_+ & \mathbf{0} \\ \boldsymbol{V}_{-\sigma} & \mathbf{0} & \boldsymbol{R}_- \end{bmatrix}. \tag{29}$$

The matrix $\mathcal{P}(\boldsymbol{\Theta})$ is organized as follows: The first M columns (rows) refer to the diffusion states $\mathcal{S}_\sigma$, the next n columns (rows) to the states $\mathcal{S}_+$ and the last m columns (rows) to the states $\mathcal{S}_-$. Quantities related to the hitting of an upper barrier are in the following marked by "+", quantities related to the lower barrier by "-". Define the upper (+) and lower (-) first-passage time of the process Y by:

$$\tau_x^\pm(i) := \inf\{t > 0 \,|\, Y_t = 0,\ Y_0 = \mp x,\ \zeta_0 = i \in \mathcal{S}\}\,,$$

for $x \ge 0$. For $i \in \mathcal{S}_\sigma \cup \mathcal{S}_+$ and $j \in \mathcal{S}_\sigma \cup \mathcal{S}_-$, we further introduce the limiting cases $\lim_{x\to 0} \tau_x^+(i) = \tau_0^+(i) = 0$ and $\lim_{x\to 0} \tau_x^-(j) = \tau_0^-(j) = 0$, respectively. For $j \in \mathcal{S}$, the Laplace transform is given by $\{\boldsymbol{E}_\pm^{(1)}(x)\}_{ij} := \mathbb{E}\big[e^{-\int_0^{\tau_x^\pm(i)} \theta^{(\varphi_s)}\mathrm{d}s}\mathbb{1}_{\zeta_{\tau_x^\pm(i)=j}}\big]$ for $x \ge 0$, $i, j \in \mathcal{S}_\sigma \cup \mathcal{S}_+$ and $i, j \in \mathcal{S}_\sigma \cup \mathcal{S}_-$, respectively. For convenience, we also introduce the parameterization:[6]

$$\boldsymbol{E}_\pm^{(1)}(x) := \exp\left(\boldsymbol{U}_\pm^{(1)} x\right) := \exp\left(\begin{bmatrix} \boldsymbol{U}_{\sigma\sigma}^{(1)} & \boldsymbol{U}_{\sigma\pm}^{(1)} \\ \boldsymbol{U}_{\pm\sigma}^{(1)} & \boldsymbol{U}_{\pm\pm}^{(1)} \end{bmatrix} x\right), \tag{30}$$

where $\exp(\cdot)$ denotes the matrix exponential. Let us define the matrices

$$\left\{\boldsymbol{\Psi}_\pm^{(1)}\right\}_{ij} = \left\{\boldsymbol{E}_\pm^{(1)}(0)\right\}_{ij} = \mathbb{E}\left[e^{-\int_0^{\tau_0^\pm(i)} \theta^{(\varphi_s)}\mathrm{d}s}\mathbb{1}_{\zeta_{\tau_0^\pm(i)}=j}\right],$$

for $i \in \mathcal{S}$, $j \in \mathcal{S}_\sigma \cup \mathcal{S}_+$ and $j \in \mathcal{S}_\sigma \cup \mathcal{S}_-$, respectively. Note that the matrices $\boldsymbol{\Psi}_\pm^{(1)}$ have a natural interpretation. To see why this is the case, recall the definition of $\tau_0^\pm(j)$ from above. For $j \in \mathcal{S}_\sigma \cup \mathcal{S}_-$, the process Y is immediately absorbed (i.e. $\tau_0^-(j) = 0$), ending up in the same state $\zeta_{\tau_0^-(j)} = \zeta_0 = j$. In case of an upper jump $j \in \mathcal{S}_+$, absorption is uncertain. Proposition 6.1 derives a Sylvester equation to obtain the matrices $\boldsymbol{U}_\pm^{(1)}$ and $\boldsymbol{\Psi}_\pm^{(1)}$.

Proposition 6.1 (Sylvester equations: Exponential time $\tau_{1,\mu}$)**.** *The matrices* ($\boldsymbol{\Psi}_-^{(1)}$, $\boldsymbol{\Psi}_+^{(1)}$, $\boldsymbol{U}_-^{(1)}$, $\boldsymbol{U}_+^{(1)}$) *are uniquely defined by a system of Sylvester equations*

$$\Upsilon\left(\boldsymbol{U}_-^{(1)},\ \boldsymbol{\Psi}_-^{(1)},\ \mathcal{P}(\boldsymbol{\Theta}),\ \hat{\boldsymbol{\Sigma}},\ \hat{\boldsymbol{D}}\right) = \mathbf{0},$$
$$\Upsilon\left(-\boldsymbol{U}_+^{(1)},\ \boldsymbol{\Psi}_+^{(1)},\ \mathcal{P}(\boldsymbol{\Theta}),\ \hat{\boldsymbol{\Sigma}},\ \hat{\boldsymbol{D}}\right) = \mathbf{0}\,, \tag{31}$$

where

$$\Upsilon\left(\boldsymbol{U},\ \boldsymbol{\Psi},\ \mathcal{P},\ \hat{\boldsymbol{\Sigma}},\ \hat{\boldsymbol{D}}\right) = \frac{1}{2}\hat{\boldsymbol{\Sigma}}\cdot\boldsymbol{\Psi}\cdot\boldsymbol{U}^2 + \hat{\boldsymbol{D}}\cdot\boldsymbol{\Psi}\cdot\boldsymbol{U} + \mathcal{P}\cdot\boldsymbol{\Psi}\,,$$

$$\boldsymbol{\Psi}_-^{(1)} = \begin{bmatrix} \boldsymbol{I}_M & \mathbf{0} \\ \boldsymbol{\Psi}_{+\sigma}^{(1)} & \boldsymbol{\Psi}_{+-}^{(1)} \\ \mathbf{0} & \boldsymbol{I}_m \end{bmatrix},\ \boldsymbol{\Psi}_+^{(1)} = \begin{bmatrix} \boldsymbol{I}_M & \mathbf{0} \\ \mathbf{0} & \boldsymbol{I}_n \\ \boldsymbol{\Psi}_{-\sigma}^{(1)} & \boldsymbol{\Psi}_{-+}^{(1)} \end{bmatrix},$$

$$\hat{\boldsymbol{\Sigma}} = \begin{bmatrix} \boldsymbol{\Sigma}^2 & \mathbf{0} & \mathbf{0} \\ \mathbf{0} & \mathbf{0} & \mathbf{0} \\ \mathbf{0} & \mathbf{0} & \mathbf{0} \end{bmatrix},\ \hat{\boldsymbol{D}} = \begin{bmatrix} \boldsymbol{D} & \mathbf{0} & \mathbf{0} \\ \mathbf{0} & \boldsymbol{I}_n & \mathbf{0} \\ \mathbf{0} & \mathbf{0} & -\boldsymbol{I}_m \end{bmatrix}.$$

Proof. e.g. Ivanovs (2010). In case of an upper jump $j \in \mathcal{S}_+$, absorption is uncertain and parameterized via $[\boldsymbol{\Psi}_{+\sigma}^{(1)}\ \boldsymbol{\Psi}_{+-}^{(1)}]$ in $\boldsymbol{\Psi}_-^{(1)}$. □

Various numerical procedures are available in the literature to solve (31) and obtain $\boldsymbol{\Psi}_\pm^{(1)}$ and $\boldsymbol{U}_\pm^{(1)}$ numerically, see for instance Gardiner, Laub, Amato, & Moler (1992), Breuer (2008) and Nguyen & Poloni (2016). We can further relate the Sylvester Eq. (31) to the matrix Wiener-Hopf factorization, see Remark 6.2 and Jiang & Pistorius (2008).

Remark 6.2 (Relation to matrix Wiener-Hopf factorization)**.** In, for example, Jiang & Pistorius (2008), the Laplace transform of the first-passage time for a Markov-modulated Brownian motion with two-sided phase type jumps is expressed in terms of the so-called matrix Wiener-Hopf factorization $(\boldsymbol{W}^+, \boldsymbol{G}^+, \boldsymbol{W}^-, \boldsymbol{G}^-)$. This factorization is obtained from (31) in Proposition 6.1 by simple matrix permutation operations.[7]

6.1.2. Erlang time $\tau_{N,\mu}$

Recall that an Erlang random variable with parameters $\mu > 0$ and $N \in \mathbb{N}$ has the same distribution as the sum of N independent exponential random variables with parameter μ, see also (1). In the following, we use a second phase $e_t \in \{1, 2, \dots, N\}$ denoting the so-called Erlangization interval. The length of each Erlangization interval is an $\mathrm{Exp}(\mu)$ random variable that ticks in the

[6] The dimension of these matrices are as follows: $\boldsymbol{U}_{\sigma\sigma}^{(k)} \in \mathbb{R}^{M\times M}$, $\boldsymbol{U}_{\sigma-}^{(k)} \in \mathbb{R}^{M\times m}$, $\boldsymbol{U}_{-\sigma}^{(k)} \in \mathbb{R}^{m\times M}$, $\boldsymbol{U}_{--}^{(k)} \in \mathbb{R}^{m\times m}$, $\boldsymbol{U}_{\sigma+}^{(k)} \in \mathbb{R}^{M\times n}$, $\boldsymbol{U}_{+\sigma}^{(k)} \in \mathbb{R}^{n\times M}$, $\boldsymbol{U}_{++}^{(k)} \in \mathbb{R}^{n\times n}$.

[7] The relation is obtained by exchanging the rows and columns of the upper jump states and the diffusion states. This is done via the permutation matrices:

$$\boldsymbol{P}_{+\sigma} := \begin{bmatrix} \mathbf{0} & \boldsymbol{I}_n \\ \boldsymbol{I}_M & \mathbf{0} \end{bmatrix},\quad \boldsymbol{P} := \begin{bmatrix} \boldsymbol{P}_{+\sigma} & \mathbf{0} \\ \mathbf{0} & \boldsymbol{I}_m \end{bmatrix}$$

and the transpose $\boldsymbol{P}'_{+\sigma}$, $\boldsymbol{P}'$. Comparing to (4.2) in Jiang & Pistorius (2008), we have that $\boldsymbol{W}^+ = \boldsymbol{P}\cdot\boldsymbol{\Psi}_+^{(1)}\cdot\boldsymbol{P}'_{+\sigma}$, $\boldsymbol{G}^+ = \boldsymbol{P}_{+\sigma}\cdot\boldsymbol{U}_+^{(1)}\cdot\boldsymbol{P}'_{+\sigma}$, $\boldsymbol{W}^- = \boldsymbol{P}\cdot\boldsymbol{\Psi}_-^{(1)}$, $\boldsymbol{G}^- = \boldsymbol{U}_-^{(1)}$, and $\boldsymbol{Q}_u = \boldsymbol{P}\cdot\mathcal{P}(\Theta)\cdot\boldsymbol{P}'$. The drift and volatility matrix are also transformed to $\boldsymbol{P}\cdot\hat{\boldsymbol{D}}\cdot\boldsymbol{P}'$ and $\boldsymbol{P}\cdot\hat{\boldsymbol{\Sigma}}\cdot\boldsymbol{P}'$, respectively.

diffusion states $\varphi_t = \zeta_{\mathcal{T}^{-1}(t)} \in \mathcal{S}_\sigma$ only. After the N-th Erlangization interval, the process is stopped. Given the subgenerator $\mathcal{P}(\boldsymbol{\Theta})$ in (29) and the matrix $\boldsymbol{\Xi}$ of the same size, we define the new generator matrix of the process Y as

$$G = \left[\begin{array}{c|ccc} 0 & \mathbf{0} & \mathbf{0} & \mathbf{0} \\ \hline \mathbf{0} & & & \\ \cdots & & & \\ \mathbf{0} & & \widetilde{\mathcal{P}}(\boldsymbol{\Theta}) & \\ \mu \boldsymbol{I}_M & & & \\ \mathbf{0} & & & \end{array}\right], \quad \text{where} \tag{32}$$

$$\widetilde{\mathcal{P}}(\boldsymbol{\Theta}) := \begin{bmatrix} \mathcal{P}(\boldsymbol{\Theta}) & \boldsymbol{\Xi} & \mathbf{0} & \cdots & \mathbf{0} \\ \mathbf{0} & \mathcal{P}(\boldsymbol{\Theta}) & \boldsymbol{\Xi} & \cdots & \vdots \\ \vdots & \cdots & \ddots & \ddots & \boldsymbol{\Xi} \\ \mathbf{0} & \mathbf{0} & \cdots & \cdots & \mathcal{P}(\boldsymbol{\Theta}) \end{bmatrix},$$

$$\boldsymbol{\Xi} := \begin{bmatrix} \mu \boldsymbol{I}_M & \mathbf{0} & \mathbf{0} \\ \mathbf{0} & \mathbf{0} & \mathbf{0} \\ \mathbf{0} & \mathbf{0} & \mathbf{0} \end{bmatrix}. \tag{33}$$

Informally stated, the resulting Markov chain moves after an exponential time $\tau_{1,\mu}$ to a new Erlang interval. After N such intervals, the process is absorbed. A first-passage can take place in any of the Erlangization intervals $k \in \{1, \ldots, N\}$. We are interested in the first passage transform matrices $\boldsymbol{E}_\pm^{(k)}$ such that

$$\left\{\boldsymbol{E}_\pm^{(k)}(x)\right\}_{ij} = \mathbb{E}\left[e^{-\int_0^{\tau_x^\pm(i)} \theta(\varphi_s) ds} \mathbb{1}_{(\varphi_{\tau_x^\pm(i)}, e_{\tau_x^\pm(i)})=(j,k)} \,\middle|\, (\varphi_0, e_0) = (i, 1)\right], \tag{34}$$

for $x \geq 0$, $i, j \in \mathcal{S}_\sigma \cup \mathcal{S}_+$ and $i, j \in \mathcal{S}_\sigma \cup \mathcal{S}_-$, respectively. The desired blocks $\boldsymbol{E}_\pm^{(k)}(x)$ from (34) that constitute the matrix $\boldsymbol{E}_\pm(x)$ are obtained by a matrix exponential:

$$\boldsymbol{E}_\pm(x) = \exp\left(\widetilde{\boldsymbol{U}}_\pm x\right) = \begin{bmatrix} \boldsymbol{E}_\pm^{(1)}(x) & \boldsymbol{E}_\pm^{(2)}(x) & \boldsymbol{E}_\pm^{(3)}(x) & \cdots & \boldsymbol{E}_\pm^{(N)}(x) \\ \mathbf{0} & \boldsymbol{E}_\pm^{(1)}(x) & \boldsymbol{E}_\pm^{(2)}(x) & \cdots & \boldsymbol{E}_\pm^{(N-1)}(x) \\ \mathbf{0} & \mathbf{0} & \boldsymbol{E}_\pm^{(1)}(x) & \cdots & \boldsymbol{E}_\pm^{(N-2)}(x) \\ \vdots & \vdots & \vdots & \ddots & \vdots \\ \mathbf{0} & \mathbf{0} & \mathbf{0} & \cdots & \boldsymbol{E}_\pm^{(1)}(x) \end{bmatrix}, \tag{35}$$

where the $\mathbb{R}^{(M+m)\times(M+m)}$ matrices $(\boldsymbol{U}_-^{(1)}, \boldsymbol{U}_-^{(2)},\ldots,\boldsymbol{U}_-^{(N)})$ and the $\mathbb{R}^{(M+n)\times(M+n)}$ matrices $(\boldsymbol{U}_+^{(1)}, \boldsymbol{U}_+^{(2)},\ldots,\boldsymbol{U}_+^{(N)})$ are placed in two Toeplitz matrices:

$$\widetilde{\boldsymbol{U}}_\pm = \begin{bmatrix} \boldsymbol{U}_\pm^{(1)} & \boldsymbol{U}_\pm^{(2)} & \boldsymbol{U}_\pm^{(3)} & \cdots & \boldsymbol{U}_\pm^{(N)} \\ \mathbf{0} & \boldsymbol{U}_\pm^{(1)} & \boldsymbol{U}_\pm^{(2)} & \cdots & \boldsymbol{U}_\pm^{(N-1)} \\ \mathbf{0} & \mathbf{0} & \boldsymbol{U}_\pm^{(1)} & \cdots & \boldsymbol{U}_\pm^{(N-2)} \\ \vdots & \vdots & \vdots & \ddots & \vdots \\ \mathbf{0} & \mathbf{0} & \mathbf{0} & \cdots & \boldsymbol{U}_\pm^{(1)} \end{bmatrix}. \tag{36}$$

It will turn out that, for $k = 2, 3, \ldots, N$, we obtain the matrix structure $\boldsymbol{U}_\pm^{(k)} = \begin{bmatrix} \boldsymbol{U}_{\sigma\sigma}^{(k)} & \boldsymbol{U}_{\sigma\pm}^{(k)} \\ \mathbf{0} & \mathbf{0} \end{bmatrix}$ with matrices that are of the same size as $\boldsymbol{U}_\pm^{(1)}$ in (29). Proposition 6.3 shows how to obtain $\widetilde{\boldsymbol{U}}_\pm$ in (36).

Proposition 6.3 (Sylvester equations: Erlang time. $\tau_{N,\mu}$**)** *For $k = 2, \ldots, n$, introduce*

$$\boldsymbol{\Psi}_-^{(k)} = \begin{bmatrix} \mathbf{0}_M & \mathbf{0} \\ \boldsymbol{\Psi}_{+\sigma}^{(k)} & \boldsymbol{\Psi}_{+-}^{(k)} \\ \mathbf{0} & \mathbf{0}_m \end{bmatrix}, \quad \boldsymbol{\Psi}_+^{(k)} = \begin{bmatrix} \mathbf{0}_M & \mathbf{0} \\ \mathbf{0} & \mathbf{0}_n \\ \boldsymbol{\Psi}_{-\sigma}^{(k)} & \boldsymbol{\Psi}_{-+}^{(k)} \end{bmatrix}$$

and use this to define the Toeplitz matrices:

$$\widetilde{\boldsymbol{\Psi}}_\pm = \begin{bmatrix} \boldsymbol{\Psi}_\pm^{(1)} & \boldsymbol{\Psi}_\pm^{(2)} & \boldsymbol{\Psi}_\pm^{(3)} & \cdots & \boldsymbol{\Psi}_\pm^{(N)} \\ \mathbf{0} & \boldsymbol{\Psi}_\pm^{(1)} & \boldsymbol{\Psi}_\pm^{(2)} & \cdots & \boldsymbol{\Psi}_\pm^{(N-1)} \\ \mathbf{0} & \mathbf{0} & \boldsymbol{\Psi}_\pm^{(1)} & \cdots & \boldsymbol{\Psi}_\pm^{(N-2)} \\ \vdots & \vdots & \vdots & \ddots & \vdots \\ \mathbf{0} & \mathbf{0} & \mathbf{0} & \cdots & \boldsymbol{\Psi}_\pm^{(1)} \end{bmatrix}. \tag{37}$$

The matrices $\widetilde{\boldsymbol{U}}_-$, $\widetilde{\boldsymbol{\Psi}}_-$, $\widetilde{\boldsymbol{U}}_+$ and $\widetilde{\boldsymbol{\Psi}}_+$ are determined via

$$\Upsilon\left(\widetilde{\boldsymbol{U}}_-, \widetilde{\boldsymbol{\Psi}}_-, \widetilde{\mathcal{P}}(\boldsymbol{\Theta}), \widetilde{\boldsymbol{\Sigma}}, \widetilde{\boldsymbol{D}}\right) = \mathbf{0},$$
$$\Upsilon\left(-\widetilde{\boldsymbol{U}}_+, \widetilde{\boldsymbol{\Psi}}_+, \widetilde{\mathcal{P}}(\boldsymbol{\Theta}), \widetilde{\boldsymbol{\Sigma}}, \widetilde{\boldsymbol{D}}\right) = \mathbf{0}, \tag{38}$$

where $\Upsilon(\boldsymbol{U}, \boldsymbol{\Psi}, \mathcal{P}, \widehat{\boldsymbol{\Sigma}}, \widehat{\boldsymbol{D}})$ is as in (31), $\widetilde{\boldsymbol{\Sigma}} := \boldsymbol{I}_N \otimes \widehat{\boldsymbol{\Sigma}}$, $\widetilde{\boldsymbol{D}} := \boldsymbol{I}_N \otimes \widehat{\boldsymbol{D}}$ and $\otimes$ denotes the Kronecker product.

Proof. e.g. Ivanovs (2010). □

To solve the system (38), it is convenient to write the matrices in their block structure. With some simplifications, Lemma 6.4 allows to conveniently obtain the different matrices iteratively solving a series of Sylvester equations, see also Deelstra et al. (2020).

Lemma 6.4 (Iterative solution of Proposition 6.3)**.** *Introduce, for $k = 2, 3, \ldots, N$, the matrices $\boldsymbol{Z}_\pm^{(k)} = \begin{bmatrix} \boldsymbol{U}_{\sigma\sigma}^{(k)} & \boldsymbol{U}_{\sigma\pm}^{(k)} \\ \boldsymbol{\Psi}_{\mp\sigma}^{(k)} & \boldsymbol{\Psi}_{\mp\pm}^{(k)} \end{bmatrix}$.*

For $k = 2$, we obtain $\boldsymbol{Z}_\pm^{(2)}$ as the unique solution of the Sylvester equation

$$\begin{bmatrix} \boldsymbol{U}_{\sigma\sigma}^{(1)} \mp 2\boldsymbol{\Sigma}^{-2}\boldsymbol{D} & 2\boldsymbol{\Sigma}^{-2}\boldsymbol{W}_{\sigma\mp} \\ \boldsymbol{\Psi}_{\mp\sigma}^{(1)} & \boldsymbol{R}_\mp \end{bmatrix} \boldsymbol{Z}_\pm^{(2)} + \boldsymbol{Z}_\pm^{(2)} \begin{bmatrix} \boldsymbol{U}_{\sigma\sigma}^{(1)} & \boldsymbol{U}_{\sigma\pm}^{(1)} \\ \boldsymbol{U}_{\pm\sigma}^{(1)} & \boldsymbol{U}_{\pm\pm}^{(1)} \end{bmatrix}$$
$$= -\begin{bmatrix} 2\mu\boldsymbol{\Sigma}^{-2} & \mathbf{0} \\ \mathbf{0} & \mathbf{0} \end{bmatrix}, \tag{39}$$

and finally, for $k \geq 3$, we can uniquely solve for $\boldsymbol{Z}_\pm^{(k)}$ by the Sylvester equation

$$\begin{bmatrix} \boldsymbol{U}_{\sigma\sigma}^{(1)} \mp 2\boldsymbol{\Sigma}^{-2}\boldsymbol{D} & 2\boldsymbol{\Sigma}^{-2}\boldsymbol{W}_{\sigma\mp} \\ \boldsymbol{\Psi}_{\mp\sigma}^{(1)} & \boldsymbol{R}_\mp \end{bmatrix} \boldsymbol{Z}_\pm^{(k)} + \boldsymbol{Z}_\pm^{(k)} \begin{bmatrix} \boldsymbol{U}_{\sigma\sigma}^{(1)} & \boldsymbol{U}_{\sigma\pm}^{(1)} \\ \boldsymbol{U}_{\pm\sigma}^{(1)} & \boldsymbol{U}_{\pm\pm}^{(1)} \end{bmatrix}$$
$$+ \sum_{l=2}^{k-1} \begin{bmatrix} \boldsymbol{U}_{\sigma\sigma}^{(l)} \boldsymbol{U}_{\sigma\sigma}^{(k-l+1)} & \boldsymbol{U}_{\sigma\sigma}^{(l)} \boldsymbol{U}_{\sigma\pm}^{(k-l+1)} \\ \boldsymbol{\Psi}_{\mp\sigma}^{(l)} \boldsymbol{U}_{\sigma\sigma}^{(k-l+1)} & \boldsymbol{\Psi}_{\mp\sigma}^{(l)} \boldsymbol{U}_{\sigma\pm}^{(k-l+1)} \end{bmatrix} = \begin{bmatrix} \mathbf{0} & \mathbf{0} \\ \mathbf{0} & \mathbf{0} \end{bmatrix}. \tag{40}$$

Proof. See Appendix C. □

Once the matrices $\boldsymbol{\Psi}_\pm^{(1)}$ and $\boldsymbol{U}_\pm^{(1)}$ are known, the matrices $\boldsymbol{\Psi}_\pm^{(k)}$ and $\boldsymbol{U}_\pm^{(k)}$, $k \geq 2$, are easily obtained by solving the Sylvester equations (39)–(40), see, for example, Gardiner et al. (1992) for details on a numerically efficient implementation. For simple cases, it is possible to solve the Sylvester equations analytically, see Example 6.6.

6.2. Digital GMDB

In this section, we consider the pricing of digital GMDBs that pay one unit of currency if the risky asset S_t drops below (exceeds) the lower (upper) level B (H) before time $\tau_{N,\mu}$. The time-0 value of these products is

$$P_-^{DG}(S_0, B, \mu, N, \boldsymbol{\pi}) = \mathbb{E}\left[e^{-\int_0^{\tau_{N,\mu}} \theta(\varphi_s) ds} \mathbb{1}_{S_0 e^{m_{\tau_{N,\mu}}} < B}\right], \tag{41}$$

$$P_+^{DG}(S_0, H, \mu, N, \boldsymbol{\pi}) = \mathbb{E}\left[e^{-\int_0^{\tau_{N,\mu}} \theta(\varphi_s) ds} \mathbb{1}_{S_0 e^{M_{\tau_{N,\mu}}} > H}\right]. \tag{42}$$

The values of digital options $P_-^{DG}(S_0, B, \mu, N, \boldsymbol{\pi})$ and $P_+^{DG}(S_0, H, \mu, N, \boldsymbol{\pi})$ are determined by:

(1) Use Propositions 6.1 and Lemma 6.4 to determine ($\boldsymbol{U}_{\pm}^{(1)}$, $\boldsymbol{U}_{\pm}^{(2)}$,...,$\boldsymbol{U}_{\pm}^{(N)}$) to obtain $\tilde{\boldsymbol{U}}_{\pm}$ via (36) and $\boldsymbol{E}_{\pm}^{(k)}$ via (35). We can decompose the matrices $\boldsymbol{E}_{\pm}^{(k)}$ as follows:

$$\boldsymbol{E}_{\pm}^{(k)}(x) = \begin{bmatrix} \boldsymbol{E}_{\sigma\sigma}^{(k)}(x) & \boldsymbol{E}_{\sigma\pm}^{(k)}(x) \\ \boldsymbol{E}_{\pm\sigma}^{(k)}(x) & \boldsymbol{E}_{\pm\pm}^{(k)}(x) \end{bmatrix}. \tag{43}$$

(2) Using (43), Proposition 6.5 gives the value of digital options in analytic form.

Note that the matrices $\cdot_+$ are used for an upper barrier digital option $P_+^{DG}(S_0, H, \mu, N, \boldsymbol{\pi})$ while the matrices $\cdot_-$ are used for $P_-^{DG}(S_0, B, \mu, N, \boldsymbol{\pi})$.

Proposition 6.5 (Digital GMDBs)**.** *The value of a digital option (41) with a risky asset S following dynamics (2), barrier level $B < S_0$ and Erlang-distributed payoff time $T_x = \tau_{N,\mu}$ is*

$$P_-^{DG}(S_0, B, \mu, N, \boldsymbol{\pi}) = \boldsymbol{\pi} \sum_{k=1}^{N} \begin{bmatrix} \boldsymbol{E}_{\sigma\sigma}^{(k)}(s_0 - b) & \boldsymbol{E}_{\sigma-}^{(k)}(s_0 - b) \end{bmatrix} \begin{bmatrix} \boldsymbol{v}_{\sigma}^{(N-k+1)} \\ \boldsymbol{v}_{-}^{(N-k+1)} \end{bmatrix}, \tag{44}$$

where $s_0 := \ln(S_0)$ and $b := \ln(B)$. With $\boldsymbol{\Psi}(\beta, \boldsymbol{\Theta})$ as in Lemma 3.1:

$$\left(\boldsymbol{v}_{\sigma}^{(N-k+1)}\right)_{j \in \mathcal{S}_\sigma} = \mathbb{E}\left[e^{-\int_0^{\tau_{N,\mu}} \theta^{(\varphi_s)} ds} \,\middle|\, (\zeta_0, e_0) = (j, k) \right] = \mu^{N-k+1} (\mu \boldsymbol{I}_M - \boldsymbol{\Psi}(0, \boldsymbol{\Theta}))^{-N+k-1} \boldsymbol{1}, \tag{45}$$

$$\left(\boldsymbol{v}_{\pm}^{(N-k+1)}\right)_{j \in \mathcal{S}_\pm} = \mathbb{E}\left[e^{-\int_0^{\tau_{N,\mu}} \theta^{(\varphi_s)} ds} \,\middle|\, (\zeta_0, e_0) = (s_j^{\pm}, k) \right] = (-\boldsymbol{R}_{\pm})^{-1} \boldsymbol{V}_{\pm\sigma} \boldsymbol{v}_{\sigma}^{(N-k+1)}, \tag{46}$$

For (42), i.e. an upper barrier $H > S_0$ and $h := \ln(H)$, we obtain

$$P_+^{DG}(S_0, H, \mu, N, \boldsymbol{\pi}) = \boldsymbol{\pi} \sum_{k=1}^{N} \begin{bmatrix} \boldsymbol{E}_{\sigma\sigma}^{(k)}(h - s_0) & \boldsymbol{E}_{\sigma+}^{(k)}(h - s_0) \end{bmatrix} \begin{bmatrix} \boldsymbol{v}_{\sigma}^{(N-k+1)} \\ \boldsymbol{v}_{+}^{(N-k+1)} \end{bmatrix}. \tag{47}$$

Proof. See also Deelstra et al. (2020)[8]. Note that in (46), we also allow for the possibility of initial jump states, that is $\zeta_0 \in \mathcal{S}$. For the discount factor, we can use Lemma 3.1 and 5.1 to get $\left(\boldsymbol{v}_{\sigma}^{(N-k+1)}\right)_{j \in \mathcal{S}_\sigma} := \phi_{\tau_{N-k+1,\mu}}^{(j)}(0)$. Given that the current state is a jump state, we further get (46). Using this, we obtain for $x = s_0 - b > 0$ and $j \in \mathcal{S}_\sigma$:

$$\begin{aligned} P_-^{DG}\big(S_0, B, \mu, N, \boldsymbol{e}_j\big) &= \mathbb{E}\left[e^{-\int_0^{\tau_{N,\mu}} \theta^{(\varphi_s)} ds} \mathbb{1}_{S_0 e^{m_{\tau_{N,\mu}}} < B} \,\middle|\, Y_0 = x,\ (\zeta_0, e_0) = (j, 1) \right] \\ &= \sum_{k=1}^{N} \sum_{i \in \mathcal{S}_\sigma \cup \mathcal{S}_-} \mathbb{E}\Big[e^{-\int_0^{\tau_{N,\mu}} \theta^{(\varphi_s)} ds} \mathbb{1}_{(\zeta_{\tau_x^-(j)}, e_{\tau_x^-(j)}) = (i,k)} \,\Big|\, \\ &\qquad Y_0 = x,\ (\zeta_0, e_0) = (j, 1) \Big] \\ &= \sum_{k=1}^{N} \sum_{i \in \mathcal{S}_\sigma \cup \mathcal{S}_-} \mathbb{E}\Big[e^{-\int_0^{\tau_x^-(j)} \theta^{(\varphi_s)} ds} \mathbb{1}_{(\zeta_{\tau_x^-(j)}, e_{\tau_x^-(j)}) = (i,k)} \,\Big|\, \\ &\qquad Y_0 = x,\ (\zeta_0, e_0) = (j, 1) \Big] \\ &\quad \cdot \mathbb{E}\left[e^{-\int_{\tau_x^-(j)}^{\tau_{N,\mu}} \theta^{(\varphi_s)} ds} \,\middle|\, (\zeta_{\tau_x^-(j)}, e_{\tau_x^-(j)}) = (i, k) \right] \\ &= \boldsymbol{e}_j \sum_{k=1}^{N} \begin{bmatrix} \boldsymbol{E}_{\sigma\sigma}^{(k)}(s_0 - b) & \boldsymbol{E}_{\sigma-}^{(k)}(s_0 - b) \end{bmatrix} \begin{bmatrix} \boldsymbol{v}_{\sigma}^{(N-k+1)} \\ \boldsymbol{v}_{-}^{(N-k+1)} \end{bmatrix}, \end{aligned}$$

where, in the last step, we used the memoryless property of the exponential distribution. □

We look at Proposition 6.5 in the example of Kou's model and an exponential death time $\tau_{1,\mu}$. In this case, the Sylvester Eq. (31) can be solved analytically. Example 6.6 provides the details and links our result to Gerber et al. (2013).

Example 6.6 (Kou's model (continued))**.** Recall Kou's model from Example 3.3 ($M = 1$) and assume that the interest rate is constant, that is $\theta^{(\varphi_t)} = r$ for all $t \geq 0$. The roots of $\boldsymbol{\Psi}(\beta, \boldsymbol{\Theta}) = \mu$ in (14) are given by $-\infty < \alpha_1 < \alpha_2 < 0 < \beta_1 < \beta_2 < \infty$. We can solve the Sylvester Eq. (31) in this case analytically (see the Appendix for the calculations):

$$\boldsymbol{U}_+^{(1)} = \begin{bmatrix} \alpha_+ - \beta_1 - \beta_2 & -\frac{\beta_1\beta_2}{\alpha_+} + \beta_1 + \beta_2 - \alpha_+ \\ \alpha_+ & -\alpha_+ \end{bmatrix}. \tag{48}$$

Assuming that we are initially in the diffusion state, we obtain with $z := h - s_0$, initial distribution on the states $\boldsymbol{\pi} = \boldsymbol{e}_1$, number of Erlangization intervals $N = 1$:[9]

$$\begin{aligned} V(z, \mu, N, \boldsymbol{\pi}) &= \boldsymbol{\pi} \begin{bmatrix} \boldsymbol{E}_{\sigma\sigma}^{(1)}(z) & \boldsymbol{E}_{\sigma+}^{(1)}(z) \end{bmatrix} \begin{bmatrix} \boldsymbol{v}_{\sigma}^{(1)} \\ \boldsymbol{v}_{+}^{(1)} \end{bmatrix} = \boldsymbol{\pi} \exp\left(\boldsymbol{U}_+^{(1)} z\right) \begin{bmatrix} \frac{\mu}{\mu+r} \\ \frac{\mu}{\mu+r} \end{bmatrix} \\ &= \boldsymbol{\pi} \exp\left(\begin{bmatrix} \alpha_+ - \beta_1 - \beta_2 & -\frac{\beta_1\beta_2}{\alpha_+} + \beta_1 + \beta_2 - \alpha_+ \\ \alpha_+ & -\alpha_+ \end{bmatrix} z \right) \\ &\quad \begin{bmatrix} \frac{\mu}{\mu+r} \\ \frac{\mu}{\mu+r} \end{bmatrix} = [1\ 0] \left(\frac{\beta_1 e^{-\beta_2 z} - \beta_2 e^{-\beta_1 z}}{\beta_1 - \beta_2} \begin{bmatrix} 1 & 0 \\ 0 & 1 \end{bmatrix} \right. \\ &\quad + \frac{e^{-\beta_2 z} - e^{-\beta_1 z}}{\beta_1 - \beta_2} \\ &\quad \left. \cdot \begin{bmatrix} \alpha_+ - \beta_1 - \beta_2 & -\frac{\beta_1\beta_2}{\alpha_+} + \beta_1 + \beta_2 - \alpha_+ \\ \alpha_+ & -\alpha_+ \end{bmatrix} \right) \begin{bmatrix} \frac{\mu}{\mu+r} \\ \frac{\mu}{\mu+r} \end{bmatrix} \\ &= \frac{\mu}{\mu + r} \left(\frac{\beta_2}{\beta_2 - \beta_1} \frac{\alpha_+ - \beta_1}{\alpha_+} e^{-\beta_1 z} + \frac{\beta_1}{\beta_2 - \beta_1} \frac{\beta_2 - \alpha_+}{\alpha_+} e^{-\beta_2 z} \right) \\ &=: \frac{\mu}{\mu + r} \left(B_1 e^{-\beta_1 z} + B_2 e^{-\beta_2 z} \right) \end{aligned}$$

with constants $B_1 := \frac{\beta_2(\alpha_+ - \beta_1)}{\alpha_+(\beta_2 - \beta_1)}$ and $B_2 := \frac{\beta_1(\beta_2 - \alpha_+)}{\alpha_+(\beta_2 - \beta_1)}$. This expression is the Laplace transform for the first-passage time in Kou's model, see Kou & Wang (2003). From this, we obtain:

$$P_+^{DG}(S_0, H, \mu, N, \boldsymbol{\pi}) = S_0 \cdot V(h - s_0, \mu, N, \boldsymbol{\pi}) = S_0 \frac{\mu}{\mu + r} \left[B_1 \left(\frac{S_0}{H}\right)^{\beta_1} + B_2 \left(\frac{S_0}{H}\right)^{\beta_2} \right].$$

[8] Remark that these results are derived in Deelstra et al. (2020) in order to obtain approximations for European digitals with a fixed horizon. In this paper, we focus first on digital GMDBs with a random payment date T_x and later on lookback GMDBs, where the pricing formulae will be useful. We therefore include a proof for completeness.

[9] In the following, we use Sylvester's formula (see Sylvester (1883)) that allows to compute the matrix exponential of a diagonalizable matrix $\boldsymbol{A}$ with distinct eigenvalues $\lambda_1, \lambda_2, \ldots, \lambda_k$:

$$\exp(\boldsymbol{A}) = \sum_{i=1}^{k} e^{\lambda_i} A_i, \tag{49}$$

where $A_i := \prod_{j=1, j \neq i}^{k} \frac{1}{\lambda_i - \lambda_j} (\boldsymbol{A} - \lambda_j \boldsymbol{I}_k)$. The eigenvalues of the matrix $\boldsymbol{U}_+^{(1)}$ are $\lambda_1 = -\beta_1$ and $\lambda_2 = -\beta_2$.

6.3. Lookback GMDBs

Finally, we study standard lookback options. The time-$\tau_{N,\mu}$ payoff of a floating-strike lookback GMDB is

$$b(\tau_{N,\mu}, S_{\tau_{N,\mu}}, M_{\tau_{N,\mu}}) = \max\left(H,\, S_0 e^{M_{\tau_{N,\mu}}}\right) - S_{\tau_{N,\mu}}\,, \tag{50}$$

where H is the initial maximum of the risky asset, see also Siu et al. (2015). Given (50), the time-0 value of this product is

$$P^{\mathrm{LB}}(S_0, B, \mu, N, \boldsymbol{\pi}) = \mathbb{E}\left[e^{-\int_0^{\tau_{N,\mu}} \theta(\varphi_s)\,\mathrm{d}s}\, b(\tau_{N,\mu}, S_{\tau_{N,\mu}}, M_{\tau_{N,\mu}})\right]. \tag{51}$$

Again, we present the different steps to obtain $P^{\mathrm{LB}}(S_0, B, \mu, N, \boldsymbol{\pi})$:

(1) Use Propositions 6.1, 6.3, Lemma 6.4 for $(\boldsymbol{U}_\pm^{(1)}, \boldsymbol{U}_\pm^{(2)},\dots,\boldsymbol{U}_\pm^{(N)})$ to obtain $\widetilde{\boldsymbol{U}}_\pm$ via (36).
(2) Determine $\boldsymbol{\nu}_\sigma^{(k)}$, $\boldsymbol{\nu}_-^{(k)}$, $\boldsymbol{\nu}_+^{(k)}$, for $k = 1, 2, \dots, N$, from (45) – (46).
(3) Proposition 6.7 expresses the price of a lookback option in analytical form.

Note that, having solved the Sylvester equations in Proposition 6.3, the price of a lookback GMDB is in analytical form – there is no need for an additional numerical integration or Laplace inversion. Proposition 6.7 gives the details.

Proposition 6.7 (Lookback GMDBs)**.** *The value of a lookback option (51) with a risky asset S following dynamics (2) and satisfying the assumption that $\tilde{\lambda}_0^+ < -1$ where $\tilde{\lambda}_0^+ := \max\{\lambda : \lambda \text{ eigenvalue of } \widetilde{\boldsymbol{U}}_+\}$, upper level $H > S_0$ and Erlang-distributed payoff time $\tau_{N,\mu}$ is*

$$P^{LB}(S_0, H, \mu, N, \boldsymbol{\pi})$$
$$= S_0 \begin{bmatrix} \boldsymbol{\pi} \\ \boldsymbol{0} \\ \cdots \\ \boldsymbol{0} \\ \boldsymbol{0} \end{bmatrix}' \left(-\left(\widetilde{\boldsymbol{U}}_+ + \boldsymbol{I}_\cdot\right)^{-1}\right) \exp\left((\widetilde{\boldsymbol{U}}_+ + \boldsymbol{I}_\cdot)z\right) \begin{bmatrix} \boldsymbol{\nu}_\sigma^{(N)} \\ \boldsymbol{\nu}_+^{(N)} \\ \cdots \\ \boldsymbol{\nu}_\sigma^{(1)} \\ \boldsymbol{\nu}_+^{(1)} \end{bmatrix}$$
$$+ H \cdot \boldsymbol{\pi}'\, \boldsymbol{\nu}_\sigma^{(N)} - S_0\,, \tag{52}$$

where $\widetilde{\boldsymbol{U}}_+$ as in (36), $s_0 := \ln(S_0)$, $z := \ln(H/S_0)$ and $\boldsymbol{\nu}_\sigma^{(k)}$, $\boldsymbol{\nu}_+^{(k)}$, $k = 1, 2, \dots, N$ as in Proposition 6.5. $\boldsymbol{I}_\cdot$ is an identity matrix with the same size as $\widetilde{\boldsymbol{U}}_+$ and $\exp(\,\cdot\,)$ denotes the matrix exponential.

Proof. The first part follows Siu et al. (2015), Theorem 3.2, to price floating-strike lookback put options for initial state $j \in \mathcal{S}_\sigma$:

$$\begin{aligned}
&P^{LB}(S_0, H, \mu, N, \boldsymbol{e}_j) \\
&= \mathbb{E}\left[e^{-\int_0^{T_x} \theta(\varphi_s)\mathrm{d}s}\left(\max\left(H, S_0 e^{M_{T_x}}\right) - S_{T_x}\right) \,\middle|\, (\zeta_0, e_0) = (j, 1)\right] \\
&= S_0 \cdot \mathbb{E}\left[e^{-\int_0^{T_x} \theta(\varphi_s)\mathrm{d}s} \max\left(e^z, e^{M_{T_x}}\right)\right) \,\middle|\, (\zeta_0, e_0) = (j, 1)\right] - S_0 \\
&= S_0 \cdot \mathbb{E}\left[e^{-\int_0^{T_x} \theta(\varphi_s)\mathrm{d}s}\left(e^{M_{T_x}} - e^z\right)\mathbb{1}_{M_{T_x} \ge z} \,\middle|\, (\zeta_0, e_0) = (j, 1)\right] \\
&\quad + S_0 e^z \cdot \mathbb{E}\left[e^{-\int_0^{T_x} \theta(\varphi_s)\mathrm{d}s} \,\middle|\, (\zeta_0, e_0) = (j, 1)\right] - S_0 \\
&= S_0 \cdot \int_z^\infty e^m \mathbb{E}\left[e^{-\int_0^{T_x} \theta(\varphi_s)\mathrm{d}s}\mathbb{1}_{M_{T_x} \ge m} \,\middle|\, (\zeta_0, e_0) = (j, 1)\right] \mathrm{d}m \\
&\quad + S_0 e^z \cdot \mathbb{E}\left[e^{-\int_0^{T_x} \theta(\varphi_s)\mathrm{d}s} \,\middle|\, (\zeta_0, e_0) = (j, 1)\right] - S_0 \\
&= S_0 \cdot \int_z^\infty e^a P_+^{DG}(1, e^a, \mu, N, \boldsymbol{\pi})\,\mathrm{d}a \\
&\quad + H \cdot \mathbb{E}\left[e^{-\int_0^{\tau_{N,\mu}} \theta(\varphi_s)\mathrm{d}s} \,\middle|\, (\zeta_0, e_0) = (j, 1)\right] - S_0\,,
\end{aligned}$$

where the last step is an application of Lemma 3.4 in Siu et al. (2015) (partial integration) and we abbreviate $z := \ln(H/S_0)$. Interestingly, it is possible to explicitly solve the integral in the latter equation. The key to this is to rewrite $P_+^{DG}(S_0, H, \mu, N, \boldsymbol{\pi})$ from Proposition 6.5 as follows:

$$\begin{aligned}
P_+^{DG}(1, e^a, \mu, N, \boldsymbol{e}_j) &= \boldsymbol{e}_j \sum_{k=1}^{N} \left[\boldsymbol{E}_{\sigma\sigma}^{(k)}(a) \quad \boldsymbol{E}_{\sigma+}^{(k)}(a)\right] \begin{bmatrix} \nu_\sigma^{(N-k+1)} \\ \nu_+^{(N-k+1)} \end{bmatrix} \\
&= \begin{bmatrix} \boldsymbol{e}_j \\ \boldsymbol{0} \\ \cdots \\ \boldsymbol{0} \\ \boldsymbol{0} \end{bmatrix}' \exp\left(\widetilde{\boldsymbol{U}}_+ a\right) \begin{bmatrix} \boldsymbol{\nu}_\sigma^{(N-1+1)} \\ \boldsymbol{\nu}_+^{(N-1+1)} \\ \cdots \\ \boldsymbol{\nu}_\sigma^{(N-N+1)} \\ \boldsymbol{\nu}_+^{(N-N+1)} \end{bmatrix},
\end{aligned}$$

where $\widetilde{\boldsymbol{U}}_+$ is as in (36). The matrix $\widetilde{\boldsymbol{U}}_+$ is a subgenerator matrix (see, for example, Definition 4.1 and Theorem 4.2 in Jiang & Pistorius (2008)). Then, with the help of Lemma 2.2, we obtain:

$$\begin{aligned}
\int_z^\infty e^a \exp\left(\widetilde{\boldsymbol{U}}_+ a\right)\mathrm{d}a &= \int_z^\infty \exp\left((\widetilde{\boldsymbol{U}}_+ + \boldsymbol{I}_\cdot)a\right)\mathrm{d}a \\
&= -\left(\widetilde{\boldsymbol{U}}_+ + \boldsymbol{I}_\cdot\right)^{-1} \exp\left((\widetilde{\boldsymbol{U}}_+ + \boldsymbol{I}_\cdot)z\right).
\end{aligned}$$

From (45), assuming β satisfying the assumptions of Lemma 5.1, recall that

$$\begin{aligned}
\left(\boldsymbol{\nu}_\sigma^{(N)}\right)_{j \in \mathcal{S}_\sigma} &= \mathbb{E}\left[e^{-\int_0^{\tau_{N,\mu}} \theta(\varphi_s)\mathrm{d}s} \,\middle|\, (\zeta_0, e_0) = (j, 1)\right] \\
&= \boldsymbol{e}_j'\left(\mu^N\left(\mu \boldsymbol{I}_M - \boldsymbol{\Psi}(0, \boldsymbol{\Theta})\right)^{-N}\right)\boldsymbol{1}\,.
\end{aligned} \tag{53}$$

With this, we obtain the value of a lookback GMDB :

$$P^{LB}(S_0, H, \mu, N, \boldsymbol{e}_j)$$
$$= S_0 \begin{bmatrix} \boldsymbol{e}_j \\ \boldsymbol{0} \\ \cdots \\ \boldsymbol{0} \\ \boldsymbol{0} \end{bmatrix}' \left(-\left(\widetilde{\boldsymbol{U}}_+ + \boldsymbol{I}_\cdot\right)^{-1}\right) \exp\left((\widetilde{\boldsymbol{U}}_+ + \boldsymbol{I}_\cdot)z\right) \begin{bmatrix} \boldsymbol{\nu}_\sigma^{(N)} \\ \boldsymbol{\nu}_+^{(N)} \\ \cdots \\ \boldsymbol{\nu}_\sigma^{(1)} \\ \boldsymbol{\nu}_+^{(1)} \end{bmatrix}$$
$$+ H \cdot \boldsymbol{e}_j'\, \boldsymbol{\nu}_\sigma^{(N)} - S_0\,.$$

□

Proposition 6.7 extends Siu et al. (2015) to a regime-dependent interest rate, an Erlang distributed death time $\tau_{N,\mu}$ and phase-type jumps. The pricing equation is explicit and does not require a Fourier inversion algorithm. The value depends solely on the solution of the Sylvester equations in Proposition 6.3. We demonstrate this in Example 6.8 on the valuation of lookback GMDBs for an exponential death time. This allows us to relate Proposition 6.7 to the results by Gerber et al. (2013) on Kou's model.

Example 6.8 (Kou's model (continued))**.** Continuing Example 6.6, we can use the term $\mathbb{E}\left[e^{-r\tau_{N,\mu}}\mathbb{1}_{M_{\tau_{N,\mu}} \ge a}\right] = V(a, \mu, N, \boldsymbol{\pi})$ to also price variable annuities with a death benefit given by a floating strike lookback option:

$$\begin{aligned}
P^{LB}(S_0, H, \mu, N, \,\cdot\,) &= S_0 \cdot \int_z^\infty e^a \mathbb{E}\left[e^{-r\tau_{N,\mu}}\mathbb{1}_{M_{\tau_{N,\mu}} \ge a}\right]\mathrm{d}a \\
&\quad + H \cdot \mathbb{E}\left[e^{-r\tau_{N,\mu}}\right] - S_0 \\
&= \frac{\mu}{\mu + r}\left[B_1 \frac{S_0^{\beta_1} H^{1-\beta_1}}{\beta_1 - 1} + B_2 \frac{S_0^{\beta_2} H^{1-\beta_2}}{\beta_2 - 1}\right] \\
&\quad + H \frac{\mu}{\mu + r} - S_0\,.
\end{aligned} \tag{54}$$

This equals (7.2) in Gerber et al. (2013).

7. Dynamic fund protection and dynamic withdrawal benefits

Let S_t be the value of a share of a mutual fund at time t and let n_t denote the number of units of the mutual fund in the investor's account. Consider first an investor buying a fund share at time 0, as well as the following "dynamic fund protection", which is assumed to be effective until the time of death and which guarantees that the account value will never fall below a fixed level L with $0 \le L \le S_0$. Indeed, in this case, as soon as the value of the account falls below the guaranteed level L, the account is credited with a sufficient number of fund units so that the value of the account remains equal to the guaranteed level L. Therefore, following Gerber et al. (2012) and Siu et al. (2015), n_t needs to be equal to

$$n_t = \max\left(1, \max_{0 \le s \le t} \frac{L}{S_s}\right). \tag{55}$$

Assuming S_t follows (2) with initial state $j \in \mathcal{S}_\sigma$ and considering an Erlang distributed time of death variable $\tau_{N,\mu}$, the expected discounted value of this contract with dynamic fund protection (denoted by DFP) equals

$$DFP(S_0, L, \mu, N, \boldsymbol{e_j}) = \left[e^{-\int_0^{\tau_{N,\mu}} \theta(\varphi_s)\mathrm{d}s} n_{\tau_{N,\mu}} S_{\tau_{N,\mu}} \,\middle|\, (\varphi_0, e_0) = (j, 1)\right]. \tag{56}$$

Let us define Q^S as an equivalent martingale measure of Q via the Radon-Nikodym derivative

$$\left.\frac{d\mathbb{Q}^S}{d\mathbb{Q}}\right|_{\mathcal{F}_t} := \frac{e^{-\int_0^t \theta(\varphi_s)\mathrm{d}s} S_t}{S_0}. \tag{57}$$

Then, one can easily check that under $\mathbb{Q}^S$ the process (X, φ) remains a Markov-modulated Brownian motion with two-sided phase-type jumps. Analogous to (11), its discounted Laplace transform is for $\beta < -\lambda_0^+ - 1$ given by

$$\begin{aligned}\boldsymbol{\Psi^S}(\beta, \boldsymbol{\Theta}) = \boldsymbol{Q^S} + \boldsymbol{D^S}\beta - \boldsymbol{\Theta} + \frac{1}{2}\boldsymbol{\Sigma}^2\beta^2 + \boldsymbol{W^S}_{\sigma-}(\beta \boldsymbol{I}_m - \boldsymbol{R^S}_-)^{-1}\boldsymbol{V^S}_{-\sigma} \\ - \boldsymbol{W^S}_{\sigma+}(\beta \boldsymbol{I}_n + \boldsymbol{R^S}_+)^{-1}\boldsymbol{V^S}_{+\sigma}\end{aligned} \tag{58}$$

for appropriate matrices $\boldsymbol{Q^S}, \boldsymbol{D^S}, \boldsymbol{W^S}, \boldsymbol{V^S}, \boldsymbol{R^S}_-$ and $\boldsymbol{R^S}_+$.

Using this new measure, Proposition 7.1 determines the value of the contract with dynamic fund protection by a matrix equation. In contrast to Siu et al. (2015), the result does not contain an integral; in contrast to Jin, Qian, Wang, & Yang (2016) no coupled system of integro-differential equations need to be solved numerically.

Proposition 7.1 (Dynamic fund protection)**.** *The value of a contract with dynamic fund protection (56) with a risky asset S following dynamics (2) and satisfying the assumption that* $\tilde{\lambda}_0^{-,S} < -1$, *where* $\tilde{\lambda}_0^{-,S} := \max\{\lambda : \lambda \text{ eigenvalue of } \widetilde{\boldsymbol{U}}_-^S\}$, *lower level* $L < S_0$ *and Erlang-distributed payoff time* $\tau_{N,\mu}$ *is given by*

$$\begin{aligned}&DFP(S_0, L, \mu, N, \boldsymbol{\pi}) \\ &= L\begin{bmatrix}\boldsymbol{\pi} \\ \boldsymbol{0} \\ \cdots \\ \boldsymbol{0} \\ \boldsymbol{0}\end{bmatrix}' \left(-\left(\widetilde{\boldsymbol{U}}_-^S + \boldsymbol{I}_.\right)^{-1}\right) \\ &\quad \exp\left(-(\widetilde{\boldsymbol{U}}_-^S + \boldsymbol{I}_.)l\right)\begin{bmatrix}\boldsymbol{1}_\sigma^{(N)} \\ \boldsymbol{1}_-^{(N)} \\ \cdots \\ \boldsymbol{1}_\sigma^{(1)} \\ \boldsymbol{1}_-^{(1)}\end{bmatrix} + S_0,\end{aligned} \tag{59}$$

where $l := \ln(L/S_0)$, $\widetilde{\boldsymbol{U}}_-^S$ *is analogous as in (36) and expressed in function of the matrices in (58).* $\boldsymbol{I}_.$ *is an identity matrix with the same size as* $\widetilde{\boldsymbol{U}}_-^S$ *and the column vector of ones is of length* $N(M+m)$.

Proof. The first part follows Siu et al. (2015), Section 3.4, to value the contract with dynamic fund protection for initial state $j \in \mathcal{S}_\sigma$:

$$\begin{aligned}&DFP(S_0, L, \mu, N, \boldsymbol{e_j}) \\ &= \mathbb{E}\Bigg[e^{-\int_0^{\tau_{N,\mu}} \theta(\varphi_s)\mathrm{d}s} \max\left(1, \max_{1 \le t \le \tau_{N,\mu}} \frac{L}{S_t}\right) S_{\tau_{N,\mu}} \,\Bigg|\, \\ &\qquad (\varphi_0, e_0) = (j, 1)\Bigg] \\ &= \mathbb{E}\left[e^{-\int_0^{\tau_{N,\mu}} \theta(\varphi_s)\mathrm{d}s}\left(\max_{1 \le t \le \tau_{N,\mu}} \frac{L}{S_t} - 1\right)_+ S_{\tau_{N,\mu}}\right) \Bigg| (\varphi_0, e_0) = (j, 1)\right] + S_0 \\ &= S_0 \cdot \mathbb{E}^S\left[\left(\max_{1 \le t \le \tau_{N,\mu}} \frac{L}{S_t} - 1\right)_+ \,\middle|\, (\varphi_0, e_0) = (j, 1)\right] + S_0,\end{aligned}$$

where the last step is an application of the change of measure in (57) and $\mathbb{E}^S[\cdot]$ denotes the expectation under $\mathbb{Q}^S$. Following the lines of Siu et al. (2015), and the proof of Proposition 6.7 easily leads to the result. □

A similar technique can be exploited in the settings of a dynamic withdrawal benefit. Indeed, let L denote a constant dividend barrier with $L \ge S_0$. An investor in a dynamical withdrawal benefit asks to receive benefits as soon as the fund reaches the level L. To achieve this, a number n_t of units of S_t are sold to keep the account value at level L. Therefore, following Gerber et al. (2012) and Siu et al. (2015), n_t needs in this setting to be equal to

$$n_t = \min\left(1, \min_{0 \le s \le t} \frac{L}{S_s}\right), \tag{60}$$

and the expected discounted value of this contract with dynamic withdrawal benefits (denoted by DWB) equals for a fund S_t that follows (2) with initial state $j \in \mathcal{S}_\sigma$ and random payoff time $T_x = \tau_{N,\mu}$

$$\begin{aligned}&DWB(S_0, L, \mu, N, \boldsymbol{e_j}) \\ &= \mathbb{E}\Bigg[e^{-\int_0^{\tau_{N,\mu}} \theta(\varphi_s)\mathrm{d}s}\left(1 - \min\left(1, \min_{0 \le s \le \tau_{N,\mu}} \frac{L}{S_s}\right)\right) S_{\tau_{N,\mu}} \,\Bigg|\, \\ &\qquad (\varphi_0, e_0) = (j, 1)\Bigg] \\ &= \mathbb{E}\left[e^{-\int_0^{\tau_{N,\mu}} \theta(\varphi_s)\mathrm{d}s}\left(1 - \min_{0 \le s \le \tau_{N,\mu}} \frac{L}{S_s}\right)_+ S_{\tau_{N,\mu}} \,\middle|\, (\varphi_0, e_0) = (j, 1)\right] \\ &= S_0 \cdot \mathbb{E}^S\left[\left(1 - \min_{0 \le s \le \tau_{N,\mu}} \frac{L}{S_s}\right)_+ \,\middle|\, (\varphi_0, e_0) = (j, 1)\right].\end{aligned} \tag{61}$$

Proposition 7.2 (Dynamic withdrawal benefit)**.** *The value of a contract with dynamic withdrawal benefit (61) with a risky asset S following dynamics (2), upper level* $L \ge S_0$ *and Erlang-distributed payoff time* $\tau_{N,\mu}$ *is given by*

$$\begin{aligned}&DWB(S_0, L, \mu, N, \boldsymbol{\pi}) \\ &= L\begin{bmatrix}\boldsymbol{\pi} \\ \boldsymbol{0} \\ \cdots \\ \boldsymbol{0} \\ \boldsymbol{0}\end{bmatrix}' \left(-\left(\widetilde{\boldsymbol{U}}_+^S - \boldsymbol{I}_.\right)^{-1}\right) \exp\left((\widetilde{\boldsymbol{U}}_+^S - \boldsymbol{I}_.)l\right)\begin{bmatrix}\boldsymbol{1}_\sigma^{(N)} \\ \boldsymbol{1}_+^{(N)} \\ \cdots \\ \boldsymbol{1}_\sigma^{(1)} \\ \boldsymbol{1}_+^{(1)}\end{bmatrix} + S_0,\end{aligned} \tag{62}$$

where $l := \ln(L/S_0)$, $\widetilde{\boldsymbol{U}}_-^S$ *analogous as in (36) expressed in function of the matrices in (58).* $\boldsymbol{I}_.$ *is an identity matrix with the same size as* $\widetilde{\boldsymbol{U}}_+^S$ *and the column vector of ones is of length* $N(M+n)$.

8. Numerical examples

In this section, we first show how a series of Erlang densities, respectively a Laguerre series expansion can be calibrated to a life table, see Section 8.1. We give brief examples on applications of European-type GMDBs (see Section 8.2) and lookback GMDBs (see Section 8.3). Throughout, we measure computation time on a 1.70 GHz PC in seconds (s).

8.1. Calibration to a life table

As in, for example, Zhang & Yong (2019), we calibrate the approximations in Sections 4.1 and 4.2 to a life table, minimizing the root mean squared error between the true data and the approximations, that is we solve

$$\operatorname{argmin}_{(B_k,n_k,\mu_k)\in\mathbb{R}^3,k=1,2,\dots,K_B}\sum_{t=1}^{L}\left|F_{T_x}(t)-\sum_{k=1}^{K_B}B_k\cdot F_{\tau_{n_k,\mu_k}}(t)\right|^2, \qquad (63)$$

subject to $\sum_{k=1}^{K_B}B_k=1$, where $F_{T_x}(t)$ is the distribution function corresponding to $f_{T_x}(t)$ and the distribution function of an Erlang random variable is $F_{\tau_{N,\mu}}(t)=1-\sum_{k=1}^{N-1}\frac{1}{k!}e^{-\mu t}(\mu t)^k$.

For the Laguerre series expansion, we do not need to perform a least-square minimization as in (63) to calibrate to a life table. Instead, we exploit that the optimal coefficients $A_k=\langle\Psi_k(t),f_{T_x}(t)\rangle$ in (16) can be computed explicitly. For a discrete life table, we obtain:

$$\begin{aligned}A_k&=\left\langle\Psi_k(t),f_{T_x}(t)\right\rangle=\sqrt{2\mu}\sum_{N=0}^{k}\binom{k}{N}\frac{(-2\mu)^N}{N!}\int_0^{\omega-x}t^Ne^{-\mu t}f_{T_x}(t)\mathrm{d}t\\&\approx\sqrt{2\mu}\sum_{N=0}^{k}\binom{k}{N}\frac{(-2\mu)^N}{N!}\sum_{t=1}^{\omega-x}t^Ne^{-\mu t}\mathbb{P}\big(T_x\in(t-1,t]\big)\\&=\sqrt{2\mu}\sum_{N=0}^{k}\binom{k}{N}\frac{(-2\mu)^N}{N!}\sum_{t=1}^{\omega-x}t^Ne^{-\mu t}\left(\frac{F_{T_x}(t-1)-F_{T_x}(t)}{F_{T_x}(0)}\right),\end{aligned}$$

see also Zhang & Yong (2019). Here, ω denotes the maximum possible age in the life table and x the (current) age of the person. The fact that Laguerre polynomials are uniformly bounded and form an orthonormal basis allows to get theoretical bounds for the approximation error. It holds that:

$$\left|f_{T_x}(t)-\tilde{f}_{T_x}(t)\right|^2\le\sum_{k=K_A+1}^{\infty}A_k^2,$$

see also Zhang & Su (2018) and Zhang & Yong (2019). We can use this result to provide an upper bound for the total calibration error $\sum_{t=1}^{L}|f_{T_x}(t)-\tilde{f}_{T_x}(t)|^2\le L\cdot\sum_{k=K_A+1}^{\infty}A_k^2$. These bounds are easy to compute as the coefficients A_k are available in closed-form. For an example, we use the life table presented in Appendix 2.A of Bowers, Gerber, Hickman, Jones, & Nesbitt (1997) with an initial age $x=30$ and $t=1,2,\dots,L$. We first follow Siu et al. (2015) and calibrate this life table for $L=25$. For the series of Erlang random variables, we impose that $n_k\le 6$. This constraint hardly affects the calibration performance. Small values of n_k will turn out to be very convenient in Sections 8.2 and 8.3. Fig. 2 (left hand side) gives the logarithm of the total mean squared errors $\sum_{t=1}^{L}|f_{T_x}(t)-\hat{f}_{T_x}(t)|^2$ and $\sum_{t=1}^{L}|f_{T_x}(t)-\tilde{f}_{T_x}(t)|^2$ over time for $K_B=5$ terms (exponential, Erlang) and $K_A=15$ terms (Laguerre expansion). In this example, we obtain (for each $t=1,2,\dots,L$) an error bound for $K_A=15$ terms of $\sum_{k=16}^{\infty}A_k^2=0.000060$ and as a comparison, error bounds for $K_A=8$ terms of $\sum_{k=9}^{\infty}A_k^2=0.00113$ and for $K_A=20$ of $\sum_{k=21}^{\infty}A_k^2=0.000011$. Assuming that the true distribution of remaining lifetime follows a parametric density like Makeham's law may allow to obtain improved error bounds with an exponential decay, see Zhang & Su (2018) and Zhang & Yong (2019) for more details.

From the left hand side of Fig. 2, we observe that the sum of Erlang densities leads to the best result. Already 5–8 terms lead to very low total mean squared errors. For the Laguerre series expansion many terms are necessary to reach the same accuracy. However, as mentioned above, the Laguerre series expansion has the advantage that it is not necessary to solve a least-squares optimization for the calibration as the coefficients are known explicitly, see Zhang & Yong (2019). The right hand side of Fig. 2 leads to a similar conclusion as the left hand side, now looking at the absolute errors $|f_{T_x}(t)-\hat{f}_{T_x}(t)|$ and $|f_{T_x}(t)-\tilde{f}_{T_x}(t)|$ for different values of $t=1,2,\dots,L$.

Solving the least-squares optimization (63) in the exponential case ($n_k=1$ for all $k=1,2,\dots,L$) turns out to be rather challenging. While, for $L=25$, we obtain a very good fit of the true life table for ages $[x,x+L]$, the tail of the life table for ages $\ge x+L$ is extrapolated very poorly (compare the red line in Fig. 3 to the black line; the parameters used here are given by (42) in Siu et al. (2015)). For higher values of L, this problem persists. As demonstrated in the left hand side of Fig. 3, this can easily lead to negative survival probabilities or a survival probability exceeding 1 (see also the Appendix of Asmussen, Laub, & Yang (2019) for a similar discussion and additional references). In contrast, Erlang distributions seem to be much more flexible to adapt to the tail of the mortality distribution, see the right hand side of Fig. 3. For later reference, we provide one parameter set in the calibration for the Erlang case with $K_B=5$ and $L=80$:

$$\begin{aligned}f_{T_x}(t)\approx{}&8.809986\cdot f_{6,0.286081}(t)+7.952294\cdot f_{6,0.190245}(t)\\&-3.305995\cdot f_{5,0.297787}(t)-13.386357\cdot f_{6,0.230329}(t)\\&+0.930071\cdot f_{3,0.193571}(t).\end{aligned} \qquad (64)$$

8.2. European-type GMDBs

Following the first part of this article (Section 5), we discuss the valuation of GMDBs whose payoff is an out-of-the-money call option with guaranteed benefit K. Following Siu et al. (2015), financial risk is modeled by a two-state regime switching Kou model as introduced in Example 2.1. We take the parameter set from Siu et al. (2015), i.e. $S_0=100$, $r=0.05$, $\sigma_1=0.1$, $\alpha_{+,1}=40$, $\alpha_{-,1}=60$, $p_1=0.25$, $\lambda_1=2$, $\sigma_2=0.4$, $\alpha_{+,2}=60$, $\alpha_{-,2}=70$, $p_2=0.75$, $\lambda_2=0.5$, and $\mathbf{Q}_0=[-0.1\ 0.1;0.2\ -0.2]$.

For our closed-form solutions, the implementation follows Examples 5.4 and 5.6 in Section 5. For the general case of regime switching jump diffusion models, Monte-Carlo simulations turn out to be rather inefficient (see Tables 2–5 in Ai & Zhang, 2022 and also Huang et al., 2014, Benth et al., 2021). That is why, we compare our suggested closed-form expression to Fourier pricing that is commonly used in related literature, see, e.g., Carr & Madan (1999) for a general introduction and Siu et al. (2015), Theorem 3.1 for an application to the regime switching Kou model. This allows us a comparison to Siu et al. (2015). In Table 1 we use the calibrated series (42) in Siu et al. (2015) of 5 exponential distributions for the distribution of remaining lifetime. Using put-call parity, we obtain GMDB put prices given the corresponding GMDB call prices (28) together with $\mathbb{E}\left[e^{-r\tau_{N,\mu}}\right]=\left(\frac{\mu}{\mu+r}\right)^N$ and $P_V(S_0)=C(S_0)-S_0+K\mathbb{E}\left[e^{-r\tau_{N,\mu}}\right]$. We compare our approximated life table to the "true price" obtained from the discrete life table of Bowers et al. (1997), linearly interpolating between successive annual grid points:

$$P_V(S_0)\approx\sum_{t=1}^{\omega-x}\left(\frac{F_{T_x}(t-1)-F_{T_x}(t)}{F_{T_x}(0)}\right)\cdot\frac{P_V(S_0,t)+P_V(S_0,t-1)}{2}, \qquad (65)$$

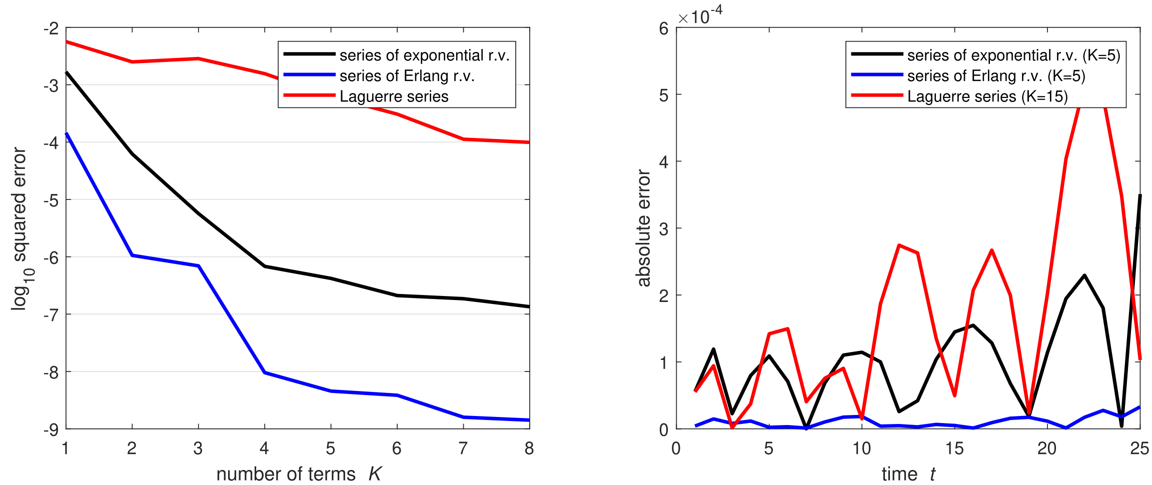

Fig. 2. Logarithmic total mean squared error (left) and absolute error for the approximation of the density $f_{T_x}(t)$ for $t = 1, 2, \dots, 25$ (right).

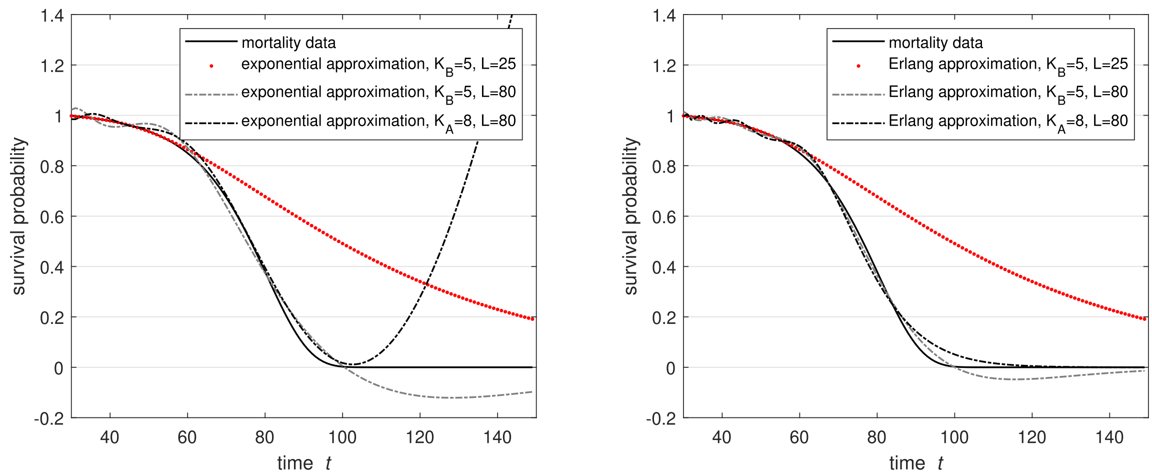

Fig. 3. True survival probability (the life table presented in Appendix 2.A of Bowers et al. (1997)) compared to its approximations, i.e. a series of exponential distributions (left hand side) for different values of K and L and a series of Erlang distributions (right).

Table 1
Values of European-type GMDBs, out-of-the-money call options following Example 5.6 and the sum-of-exponential remaining lifetime distribution (42) in Siu et al. (2015).

	Fourier price $P_V(S_0)$		time	Our price $P_V(S_0)$		time	True price $P_V(S_0)$	
	$\varphi_0 = 1$	$\varphi_0 = 2$		$\varphi_0 = 1$	$\varphi_0 = 2$		$\varphi_0 = 1$	$\varphi_0 = 2$
$K = 100$	1.1928	1.8466	0.95s	1.1928	1.8466	0.0006s	1.8848	2.7624
$K = 105$	1.3274	2.0281	0.94s	1.3274	2.0281	0.0006s	2.0823	3.0231
$K = 110$	1.4728	2.2170	0.98s	1.4728	2.2170	0.0006s	2.2912	3.2928
$K = 115$	1.6279	2.4129	1.23s	1.6279	2.4129	0.0006s	2.5113	3.5712
$K = 120$	1.7918	2.6155	0.99s	1.7918	2.6155	0.0006s	2.7421	3.8580
$K = 125$	1.9640	2.8245	1.02s	1.9640	2.8245	0.0006s	2.9831	4.1529
$K = 130$	2.1438	3.0395	1.13s	2.1438	3.0395	0.0006s	3.2338	4.4555

where the price of a put option is obtained via Fourier pricing $t = 1, 2, \dots, \omega - x$:

$$P_V(S_0) = \mathbb{E}\left[e^{-rt} \max(K - S_t, 0)\right]. \tag{66}$$

To implement Fourier pricing, we follow the fast Fourier pricing algorithm by Carr & Madan (1999) and use the Laplace transform from Lemma 5.1. We choose the number of function evaluations in the Fourier algorithm as 4096 as this allowed us to obtain all estimates in at least 5 digits of accuracy. Using Matlab, this leads to a total computation time of around 1s for five evaluations of the pricing equation. There might be ways to improve this implementation as Siu et al. (2015) report a lower number of 0.06s. Nevertheless, the closed-form expression speeds up computation significantly and obtains one price almost instantly in around 0.0006s. Both our closed-form expressions and the Fourier algorithm allow to value GMDBs with different guarantee values K at almost no additional cost.

As a second step, we use the series of Erlang distributions (64) for the remaining lifetime. Table 2 gives the result, again comparing Fourier pricing to our closed-form solutions. The increase in computation time for the closed-form solutions is mainly due to the more complicated Laurent series expansion, i.e. the coefficients (21) and (22). For the implementation, we use Matlab's `symbolic` toolbox for the derivatives. This implementation works

Table 2
Values of European-type GMDBs, out-of-the-money call options following Example 5.6 and the sum-of-Erlang remaining lifetime distribution (64).

	Fourier price $P_V(S_0)$		time	Our price $P_V(S_0)$		time	True price $P_V(S_0)$	
	$\varphi_0 = 1$	$\varphi_0 = 2$		$\varphi_0 = 1$	$\varphi_0 = 2$		$\varphi_0 = 1$	$\varphi_0 = 2$
$K = 100$	1.8476	2.7552	0.4583s	1.8476	2.7552	0.0310s	1.8848	2.7624
$K = 105$	2.0492	3.0207	0.4198s	2.0492	3.0207	0.0295s	2.0823	3.0231
$K = 110$	2.2667	3.2964	0.4346s	2.2667	3.2964	0.0295s	2.2912	3.2928
$K = 115$	2.4998	3.5819	0.4346s	2.4998	3.5819	0.0303s	2.5113	3.5712
$K = 120$	2.7474	3.8767	0.4240s	2.7474	3.8767	0.0297s	2.7421	3.8580
$K = 125$	3.0081	4.1805	0.5004s	3.0082	4.1805	0.0298s	2.9831	4.1529
$K = 130$	3.2808	4.4929	0.4463s	3.2808	4.4929	0.0291s	3.2338	4.4555

Table 3
Values of Lookback GMDBs, for different strikes K and increasing jump risk a.

	$a = 6$	$a = 10$	$a = 17$	$a = 25$	$a = 40$	$a = 70$	$a = 80$
$K = 100$	126.43	118.55	112.64	109.55	106.86	104.78	104.42
$K = 140$	127.54	119.65	113.72	110.63	107.93	105.85	105.49
$K = 180$	130.77	122.84	116.90	113.80	111.09	109.00	108.64
$K = 220$	135.35	127.39	121.42	118.31	115.60	113.51	113.15
$K = 260$	140.85	132.86	126.88	123.76	121.04	118.95	118.58
$K = 300$	147.04	139.03	133.03	129.91	127.19	125.09	124.72

quite well until around $N = 8$ – a different approach to compute (21) and (22) may significantly improve computation times for this method. The prices obtained by $K_B = 5$ Erlang distributions approximate true prices (65) much better than the exponential distributions in Table 1.

8.3. Lookback-type GMDBs

Next, we implement prices for lookback GMDBs implementing Proposition 6.7 and solving the respective Sylvester equations numerically. For the illustration, we use the phase-type jump model from Example 3.4. The distribution of remaining lifetime is chosen to be the $K_B = 5$-term Erlang distribution (64).

Table 3 gives the resulting prices for the parameter set used in Deelstra et al. (2020), i.e. $b = 3$, $c = 7.5$, $n_A = 8$, $\lambda = 10$, $q_1 = 1$, $q_2 = 4$, $\sigma_1 = 0.15$, $\sigma_2 = 0.30$, $r = 0.03$, and $S_0 = 100$. We vary the parameter a to increase jump size volatility while keeping the expected jump size constant. Each price is obtained in less than 1s. We observe that jump size volatility has a significant impact on the prices of lookback GMDBs, a much stronger effect than for the digital, vanilla and down-and-out-call GMDBs considered by Deelstra et al. (2020).

9. Conclusion

In a very general framework with regime switching returns with two-sided phase-type jumps and a remaining lifetime distribution following a series of Erlang distributions, respectively a Laguerre series expansion, we derive the Laplace transform of the returns of several vanilla and exotic GMDB contracts. Contrasting most of the related literature, our results do not rely on Fourier inversion but are either purely analytical or based on the solution of a class of affine matrix equations called Sylvester equations.

We demonstrated the usefulness of Laurent series expansions, respectively Sylvester equations for the valuation of different types of GMDBs. For European-type GMDBs the closed-form density of the terminal payoff allows us also to derive higher-order moments or quantiles to analyze and manage the contracts' risks. We believe that the techniques we use can be applied much broader, also for a fast computation of hedging weights and Greeks of GMDBs. This can be an interesting avenue for future research. Apart from this, more complex payoff features like Parisian ruin or Asian-type options may be promising extensions of this work.

10. Discussion and links to related literature

Motivated by the example of guaranteed minimum death benefits (GMDB) in insurance, we discuss the valuation and risk management of cash-flows where both level and time of payment are random. Random payment dates appear in different areas of Operations Research (OR); the randomness may be due to credit events, accidents, production failures or catastrophe- / weather-related impacts (e.g. Brigo & Vrins, 2018, Scarf, Cavalcante, & Lopes (2019)). In insurance, examples of random events include not only life insurance contracts but also reinsurance treaties, cyber-risk or operational-risk related contracts and the analysis of disruptive new technologies that affect financial cash-flows.

Our results have strong links to derivative valuation in Finance with deterministic payment dates (e.g. Cai, Song, & Kou, 2015, Hieber, 2018, Deelstra et al., 2020, Kirkby, 2023). We adapt these results to popular insurance payoffs where lookback-type payoffs are more common components of (for example) dynamic withdrawal benefits, than digital and barrier-like products covered in articles with a stronger focus on financial derivatives (e.g. Deelstra et al., 2020). Another difference is the parameter N of the Erlang distributed random time: In Carr's randomization in Finance (e.g. Carr, 1998, Deelstra et al., 2020), one chooses $N \to \infty$ while for our random payment dates values of $N \leq 10$ are sufficient. Note that the parameter N determines the number of roots in the Laurent series expansion as well as the dimension of the Sylvester equations. This parameter strongly affects the efficiency of the techniques introduced in this article.

The advantage of our approach is the fact that - in a very general model framework - we do not rely on Fourier inversion or Monte-Carlo simulation but provide computationally very convenient expressions that are either closed-form or depend on the solutions of Sylvester equations. With respect to the literature on equity-linked life insurance, we extend recent results for a Black-Scholes model or double-exponential jump diffusion model (e.g. Gerber et al., 2012, Gerber et al., 2013, Zhang & Yong, 2019, Zhang et al., 2021) to the class of regime switching Brownian motion with two-sided phase-type jumps. Laplace transforms in this model class are typically more involved as they involve matrix exponentials. We demonstrate that this class allows to still derive a Laurent series expansion of the Erlang-subordinated return density. This leads to convenient valuation formulas for European-type GMDBs, avoiding Fourier inversion algorithms as derived in, for example, Siu et al. (2015).

From a more technical perspective, we hope that the links we provide between the matrix Wiener-Hopf factorisation (e.g. Jiang & Pistorius, 2008) and Carr's randomization to techniques like the discounted density approach for GMDB analysis in insurance (e.g. Gerber et al., 2012; Gerber et al., 2015, Zhang & Yong, 2019) are interesting and foster a further exchange between different disciplines. We contribute to the tractability of regime switching models with the aim to further promote the use and application of regime switching models in OR (see also Elias et al., 2014, Hainaut, 2014, Korn et al., 2017, Jin et al., 2020).

Our analysis has limitations and contains some simplifications of reality. In further research, it may be interesting to look at for example surrender risks or Asian-type payoffs. The impact of model risk and model uncertainty for the products considered in this article may also give novel insights.

Acknowledgments

Griselda Deelstra acknowledges support from the EU Framework Programme for Research and Innovation Horizon 2020 (H2020-MSCA-ITN-2018, Project 813261, EID ABC-EU-XVA). Both authors want to thank Guy Latouche and Matthieu Simon for interesting discussions, and Matthieu Simon for sharing some of his codes. We want to thank Emanuele Borgonovo (the Editor) and four anonymous referees for many useful comments and suggestions that helped us to improve earlier versions of this manuscript.

Appendix A. Proof of Lemma 3.1

We recall from (3) that the dynamics of the MMBM can be written as

$$X_t = X_0 + \int_0^t d_{\varphi_s} \mathrm{d}s + \int_0^t \sigma_{\varphi_s} \mathrm{d}B_s + \int_0^t J^+_{\varphi_s} \mathrm{d}N_s^{\varphi_s,+} - \int_0^t J^-_{\varphi_s} \mathrm{d}N_s^{\varphi_s,-} \quad (67)$$

decomposed of a diffusion part with standard Brownian motion B_t, positive and negative jumps. Here, $N_t^{j,+}$ and $N_t^{j,-}$ are Poisson processes for the arrival of upper and lower jumps in the diffusion state $j \in \mathcal{S}_\sigma$. A jump at time t may trigger an immediate phase transition from $\varphi_{t-} = j \in \mathcal{S}_\sigma$ to $\varphi_t = k \in \mathcal{S}_\sigma$. The generator matrices $\boldsymbol{R}_+$ and $\boldsymbol{R}_-$ in (4) and (5) have negative and real-valued eigenvalues. From Proposition 17.4 in Mijatović & Pistorius (2011), we find that the expected value $\mathbb{E}[\mathbb{1}_{\varphi_t=k}\, e^{\beta J_j^+} \,|\, \varphi_{t-} = j]$ is bounded if and only if $\beta \le -\lambda_0^+$. If a jump appears at time t, we obtain from (4) and (5) and Lemma 2.2 for $\beta \le -\lambda_0^+$:

$$\begin{aligned}
&\mathbb{E}\Big[\mathbb{1}_{\varphi_t=k}\, e^{\beta J_j^+} \,\Big|\, \varphi_{t-} = j\Big]\\
&\quad= \int_0^\infty e^{\beta J_j^+} \mathrm{d}\mathbb{P}\big(J_j^+ \in \mathrm{d}x, \varphi{=}k \text{ after the jump}\big)\\
&\quad= \frac{1}{(\boldsymbol{W}_{\sigma+}\boldsymbol{1})_j} \int_0^\infty \big(\boldsymbol{W}_{\sigma+} e^{(\beta \boldsymbol{I}_n + \boldsymbol{R}_+)x} \boldsymbol{V}_{+\sigma}\big)_{jk} \mathrm{d}x\\
&\quad= -\frac{1}{(\boldsymbol{W}_{\sigma+}\boldsymbol{1})_j} \Big(\boldsymbol{W}_{\sigma+}\big(\beta \boldsymbol{I}_n + \boldsymbol{R}_+\big)^{-1} \boldsymbol{V}_{+\sigma}\Big)_{jk},
\end{aligned} \quad (68)$$

and

$$\begin{aligned}
&\mathbb{E}\Big[\mathbb{1}_{\varphi_t=k}\, e^{-\beta J_j^-} \,\Big|\, \varphi_{t-} = j\Big]\\
&\quad= \int_0^\infty e^{-\beta J_j^-} \mathrm{d}\mathbb{P}\big(J_j^- \in \mathrm{d}x, \varphi = k \text{ after the jump}\big)\\
&\quad= \frac{1}{(\boldsymbol{W}_{\sigma-}\boldsymbol{1})_j} \int_0^\infty \big(\boldsymbol{W}_{\sigma-} e^{(-\beta \boldsymbol{I}_n + \boldsymbol{R}_-)x} \boldsymbol{V}_{-\sigma}\big)_{jk} \mathrm{d}x\\
&\quad= -\frac{1}{(\boldsymbol{W}_{\sigma-}\boldsymbol{1})_j} \Big(\boldsymbol{W}_{\sigma-}\big(-\beta \boldsymbol{I}_m + \boldsymbol{R}_-\big)^{-1} \boldsymbol{V}_{-\sigma}\Big)_{jk}.
\end{aligned} \quad (69)$$

The upper or lower jumps arrive with intensity $(\boldsymbol{W}_{\sigma+}\boldsymbol{1})_j$ and $(\boldsymbol{W}_{\sigma-}\boldsymbol{1})_j$, respectively. As a first step, let us consider the case of one regime only ($M = m = n = 1$, $\varphi_t = 1, \forall t$).

$$\begin{aligned}
\phi_t^{(1)}(\beta) :&= \mathbb{E}\Big[e^{-\theta_1 t} e^{\beta X_t}\Big] = \mathbb{E}\Big[e^{-\theta_1 t} e^{\beta(d_1 t + \sigma_1 B_t) - \beta \sum_{j=1}^{N_t^{1,-}} J_1^- + \beta \sum_{j=1}^{N_t^{1,+}} J_1^+}\Big]\\
&= e^{(d_1\beta - \theta_1)t} \cdot e^{\frac{1}{2}\sigma_1^2 \beta^2 t} \cdot \mathbb{E}\Big[e^{-\beta \sum_{j=1}^{N_t^{1,-}} J_1^-}\Big] \cdot \mathbb{E}\Big[e^{\beta \sum_{j=1}^{N_t^{1,+}} J_1^+}\Big]\\
&= e^{(d_1\beta - \theta_1 + \frac{1}{2}\sigma_1^2\beta^2)t} \cdot e^{\frac{\boldsymbol{W}_{\sigma-}}{\beta - \boldsymbol{R}_-} \boldsymbol{V}_{-\sigma} t - \boldsymbol{W}_{\sigma-} t} \cdot e^{-\frac{\boldsymbol{W}_{\sigma+}}{\beta + \boldsymbol{R}_+} \boldsymbol{V}_{+\sigma} t - \boldsymbol{W}_{\sigma+} t},
\end{aligned} \quad (70)$$

where, for a Poisson process N_t with intensity λ, it holds that: $\mathbb{E}\Big[e^{\beta \sum_{j=1}^{N_t} J}\Big] = e^{\lambda t(\mathbb{E}[e^{\beta J}]-1)}$. With $\boldsymbol{Q} = -(\boldsymbol{W}_{\sigma+} + \boldsymbol{W}_{\sigma-})$, we obtain (11) and $[\boldsymbol{Q}\, \boldsymbol{W}_{\sigma+}\, \boldsymbol{W}_{\sigma-}]\boldsymbol{1} = \boldsymbol{0}$.

For the general case, apply Itô's lemma to (67) to obtain the dynamics of the discounted exponential process $Y_t := e^{-\int_0^t \theta_s \mathrm{d}s + \beta X_t}$:

$$\begin{aligned}
Y_t &= Y_0 + \int_0^t \Big(\beta d_{\varphi_s} - \theta^{(\varphi_s)} + \frac{1}{2}\beta^2 \sigma_{\varphi_s}^2\Big) Y_s \mathrm{d}s + \int_0^t \beta \sigma_{\varphi_s} Y_s \mathrm{d}B_s\\
&\quad + \int_0^t \Big(e^{\beta J^+_{\varphi_s}} - 1\Big) \mathrm{d}N_s^{\varphi_s,+} - \int_0^t \Big(e^{\beta J^-_{\varphi_s}} - 1\Big) \mathrm{d}N_s^{\varphi_s,-}.
\end{aligned} \quad (71)$$

For the case of multiple regimes ($M > 1$), introduce the vector valued process $\boldsymbol{Z}_t := (Z^{(1)}(t),\ Z^{(2)}(t), \dots, Z^{(M)}(t))'$, where $Z_t^{(j)} := \mathbb{1}_{\varphi_t=j} Y_t$ for $j \in \mathcal{S}_\sigma$. Consider a (small) time interval $\triangle t$ and assume (for now) that there are no jumps ($\boldsymbol{W}_{\sigma-} = \boldsymbol{W}_{\sigma+} = \boldsymbol{0}$). In this special case, we denote the generator matrix $\boldsymbol{Q}$ by $\boldsymbol{Q}_0$ to acknowledge that $\boldsymbol{Q}_0 \boldsymbol{1} = \boldsymbol{0}$. Following, for example, Buffington & Elliott (2002), Hieber (2017), we obtain

$$\begin{bmatrix} \mathbb{E}[Z^{(1)}_{t+\triangle t}] \\ \dots \\ \mathbb{E}[Z^{(M)}_{t+\triangle t}] \end{bmatrix} = \begin{bmatrix} \mathbb{E}[Z^{(1)}_{t}] \\ \dots \\ \mathbb{E}[Z^{(M)}_{t}] \end{bmatrix} + \int_t^{t+\triangle t} \begin{bmatrix} \mathbb{E}[Z^{(1)}_{s}] \\ \dots \\ \mathbb{E}[Z^{(M)}_{s}] \end{bmatrix}' \Big(\boldsymbol{Q}_0 + \boldsymbol{D}\beta - \boldsymbol{\Theta} + \frac{1}{2}\boldsymbol{\Sigma}^2 \beta^2\Big) \mathrm{d}s,$$

a system of differential equations that can, with $\varphi_0 = j$, be solved to

$$\begin{bmatrix} \mathbb{E}[Z^{(1)}_{t}] \\ \dots \\ \mathbb{E}[Z^{(M)}_{t}] \end{bmatrix} = \begin{bmatrix} \mathbb{E}[\mathbb{1}_{\varphi_t=1} e^{-\int_0^t \theta^{(\varphi_s)} \mathrm{d}s + \beta X_t}] \\ \dots \\ \mathbb{E}[\mathbb{1}_{\varphi_t=M} e^{-\int_0^t \theta^{(\varphi_s)} \mathrm{d}s + \beta X_t}] \end{bmatrix} = \boldsymbol{e}_j' \exp\Big(\Big(\boldsymbol{Q}_0 + \boldsymbol{D}\beta - \boldsymbol{\Theta} + \frac{1}{2}\boldsymbol{\Sigma}^2\beta^2\Big)t\Big).$$

We refer the reader to Buffington & Elliott (2002) for more details. Defining the random occupation time in $[0,t]$ in state j by $T_j(t) = \int_0^t \mathbb{1}_{\varphi_s=j} \mathrm{d}s$, $\boldsymbol{T}(t) := (T_1(t), T_2(t), \dots, T_M(t))$ and $\boldsymbol{\zeta} := (\zeta^{(1)}, \zeta^{(2)}, \dots, \zeta^{(M)})$, the result rests on:

$$\mathbb{E}\Big[\mathbb{1}_{\varphi_t=k}\, e^{\langle \boldsymbol{\zeta}, \boldsymbol{T}(t)\rangle} \,\Big|\, \varphi_0 = j\Big] = \boldsymbol{e}_j' \exp\big((\boldsymbol{Q} + \mathrm{diag}(\boldsymbol{\zeta}))t\big) \boldsymbol{e}_k, \quad (72)$$

where $\langle \cdot, \cdot \rangle$ denotes the scalar product. Next, we extend this result to upper or lower jumps in state $j \in \mathcal{S}_\sigma$ arriving at the rates $(\boldsymbol{W}_{\sigma+}\boldsymbol{1})_j$ and $(\boldsymbol{W}_{\sigma-}\boldsymbol{1})_j$, respectively. The jump might trigger a phase transition, accounted for by the matrices $\boldsymbol{V}_{+\sigma}$ and $\boldsymbol{V}_{-\sigma}$. The expected change due to jumps in state $j \in \mathcal{S}_\sigma$ are then given by:

$$\begin{aligned}
&\Big(\mathbb{P}\big(J_j{}^+ \in \mathrm{d}t\big) \cdot \mathbb{E}\Big[\mathbb{1}_{\varphi_t=k}\,(e^{\beta J_j{}^+} - 1) \,\Big|\, \varphi_{t-} = j\Big]\Big)_{jk}\\
&\quad + \Big(\mathbb{P}\big(J_j{}^- \in \mathrm{d}t\big) \cdot \mathbb{E}\Big[\mathbb{1}_{\varphi_t=k}\,(e^{-\beta J_j{}^-} - 1) \,\Big|\, \varphi_{t-} = j\Big]\Big)_{jk}\\
&\quad = \Big(\boldsymbol{W}_{\sigma-}\big(\beta \boldsymbol{I}_m - \boldsymbol{R}_-\big)^{-1} \boldsymbol{V}_{-\sigma} - \boldsymbol{W}_{\sigma+}\big(\beta \boldsymbol{I}_n + \boldsymbol{R}_+\big)^{-1} \boldsymbol{V}_{+\sigma}\\
&\quad - \mathrm{diag}\big((\boldsymbol{W}_{\sigma+} + \boldsymbol{W}_{\sigma-})\boldsymbol{1}\big)\Big) jk\, \mathrm{d}t.
\end{aligned}$$

We obtain, using that $\boldsymbol{Q}=\boldsymbol{Q}_0-\operatorname{diag}\left((\boldsymbol{W}_{\sigma+}+\boldsymbol{W}_{\sigma-})\mathbf{1}\right)$ and combining with the results from the diffusion case above:

$$\begin{bmatrix}\mathbb{E}[Z^{(1)}_{t+\triangle t}]\\ \dots\\ \mathbb{E}[Z^{(M)}_{t+\triangle t}]\end{bmatrix}=\begin{bmatrix}\mathbb{E}[Z^{(1)}_{t}]\\ \dots\\ \mathbb{E}[Z^{(M)}_{t}]\end{bmatrix}+\int_t^{t+\triangle t}\begin{bmatrix}\mathbb{E}[Z^{(1)}_{s}]\\ \dots\\ \mathbb{E}[Z^{(M)}_{s}]\end{bmatrix}'\boldsymbol{\Psi}(\beta,\boldsymbol{\Theta})\mathrm{d}s\,,$$

an equation that can be solved to:

$$\begin{bmatrix}\mathbb{E}[Z^{(1)}_{t}]\\ \dots\\ \mathbb{E}[Z^{(M)}_{t}]\end{bmatrix}=\begin{bmatrix}\mathbb{E}[\mathbb{1}_{\varphi_t=1}e^{-\int_0^t\theta^{(\varphi_s)}\mathrm{d}s+\beta X_t}]\\ \dots\\ \mathbb{E}[\mathbb{1}_{\varphi_t=M}e^{-\int_0^t\theta^{(\varphi_s)}\mathrm{d}s+\beta X_t}]\end{bmatrix}=\boldsymbol{e}_j'\exp\left(\boldsymbol{\Psi}(\beta,\boldsymbol{\Theta})t\right).$$

With this, we immediately obtain (10).

Appendix B. Proof of Lemma 5.1

Using (9) and the fact that an Erlang r.v. is the sum of N independent and identically distributed $\operatorname{Exp}(\mu)$ r.v., we obtain the vector:

$$\begin{aligned}\Phi_{\tau_{N,\mu}}(\beta):&=\begin{bmatrix}\mathbb{E}\left[e^{-\int_t^{\tau_{N,\mu}}\theta^{(\varphi_s)}\mathrm{d}s+\beta X_{\tau_{N,\mu}}}\,\Big|\,\varphi_0=1\right]\\ \dots\\ \mathbb{E}\left[e^{-\int_t^{\tau_{N,\mu}}\theta^{(\varphi_s)}\mathrm{d}s+\beta X_{\tau_{N,\mu}}}\,\Big|\,\varphi_0=M\right]\end{bmatrix}\\ &=\mathbb{E}\left[\exp\left(\boldsymbol{\Psi}(\beta,\boldsymbol{\Theta})\cdot\tau_{N,\mu}\right)\right]\mathbf{1}\\ &=\left(\mu^N\int_0^\infty\frac{t^{N-1}}{(N-1)!}e^{-\mu t}\exp\left(\boldsymbol{\Psi}(\beta,\boldsymbol{\Theta})\cdot t\right)\mathrm{d}t\right)\mathbf{1}\,.\end{aligned}$$

Note that the j-th entry of this vector is $\phi^{(j)}_{\tau_{N,\mu}}(\beta)$. The discounted characteristic function $\phi^{(j)}_{\tau_{N,\mu}}(\beta)$ exists for $\beta\le-\lambda_0^+$, see Lemma 3.1. We further apply Lemma 2.2(b) and in particular, the existence of the inverse $\left(\mu\boldsymbol{I}_M-\boldsymbol{\Psi}(\beta,\boldsymbol{\Theta})\right)^{-1}$. Applying integration by parts, we obtain

$$\Phi_{\tau_{N,\mu}}(\beta)=\mu\left(\mu\boldsymbol{I}_M-\boldsymbol{\Psi}(\beta,\boldsymbol{\Theta})\right)^{-1}\Phi_{\tau_{N-1,\mu}}(\beta)\,,\tag{73}$$

an iteration that can be solved to $\phi^{(j)}_{\tau_{N,\mu}}(\beta)=\boldsymbol{e}_j'\Phi_{\tau_{N,\mu}}(\beta)$ in (18).

Appendix C. Proof of Lemma 6.4

Let us first prove the results concerning the iteration to obtain $\boldsymbol{Z}_+^{(k)}$ for $k=2,3,\dots,N$. The idea is to solve (38) backwards, starting from the last block that equals Eq. (31) in Proposition 6.1. For the second last row, we obtain for $k=2$ that

$$\begin{aligned}\frac12\begin{bmatrix}\boldsymbol{\Sigma}^2&\mathbf{0}\\ \mathbf{0}&\mathbf{0}\\ \mathbf{0}&\mathbf{0}\end{bmatrix}&\left(\boldsymbol{U}_+^{(1)}\cdot\boldsymbol{U}_+^{(2)}+\boldsymbol{U}_+^{(2)}\cdot\boldsymbol{U}_+^{(1)}\right)\\ &-\begin{bmatrix}\boldsymbol{D}&\mathbf{0}&\mathbf{0}\\ \mathbf{0}&\boldsymbol{I}_n&\mathbf{0}\\ \mathbf{0}&\mathbf{0}&-\boldsymbol{I}_m\end{bmatrix}\left(\boldsymbol{\Psi}_+^{(1)}\cdot\boldsymbol{U}_+^{(2)}+\boldsymbol{\Psi}_+^{(2)}\cdot\boldsymbol{U}_+^{(1)}\right)\\ &+\mathcal{P}(\boldsymbol{\Theta})\cdot\boldsymbol{\Psi}_+^{(2)}+\begin{bmatrix}\mu\boldsymbol{I}_M&\mathbf{0}\\ \mathbf{0}&\mathbf{0}\\ \mathbf{0}&\mathbf{0}\end{bmatrix}=\mathbf{0}\,.\end{aligned}$$

The lowest block in this system of equation yields $\boldsymbol{U}^{(k)}_{\pm\sigma}=\boldsymbol{U}^{(k)}_{\pm\pm}=\mathbf{0}$ for $k\ge2$ (i.e. this confirms that the lowest blocks in $\boldsymbol{U}_\pm^{(k)}$ for $k\ge2$ is $\mathbf{0}$). The full system can be rewritten as follows:

$$\begin{aligned}&\begin{bmatrix}\frac12\boldsymbol{\Sigma}^2&\mathbf{0}\\ \mathbf{0}&\mathbf{0}\\ \mathbf{0}&\mathbf{0}\end{bmatrix}\begin{bmatrix}\boldsymbol{U}^{(2)}_{\sigma\sigma}&\boldsymbol{U}^{(2)}_{\sigma+}\\ \mathbf{0}&\mathbf{0}\end{bmatrix}\boldsymbol{U}_+^{(1)}+\begin{bmatrix}\mathbf{0}_M&\mathbf{0}\\ \mathbf{0}&\mathbf{0}_n\\ \boldsymbol{\Psi}^{(2)}_{-\sigma}&\boldsymbol{\Psi}^{(2)}_{-+}\end{bmatrix}\boldsymbol{U}_+^{(1)}\\ &+\begin{bmatrix}\frac12\boldsymbol{\Sigma}^2&\mathbf{0}\\ \mathbf{0}&\mathbf{0}\\ \mathbf{0}&\mathbf{0}\end{bmatrix}\begin{bmatrix}\boldsymbol{U}^{(1)}_{\sigma\sigma}&\boldsymbol{U}^{(1)}_{\sigma+}\\ \boldsymbol{U}^{(1)}_{+\sigma}&\boldsymbol{U}^{(1)}_{++}\end{bmatrix}\begin{bmatrix}\boldsymbol{U}^{(2)}_{\sigma\sigma}&\boldsymbol{U}^{(2)}_{\sigma+}\\ \mathbf{0}&\mathbf{0}\end{bmatrix}\\ &+\begin{bmatrix}\mu\boldsymbol{I}_M&\mathbf{0}\\ \mathbf{0}&\mathbf{0}\\ \mathbf{0}&\mathbf{0}\end{bmatrix}+\begin{bmatrix}\boldsymbol{D}&\mathbf{0}\\ \mathbf{0}&\boldsymbol{I}_n\\ \boldsymbol{\Psi}^{(1)}_{-\sigma}&\boldsymbol{\Psi}^{(1)}_{-+}\end{bmatrix}\begin{bmatrix}\boldsymbol{U}^{(2)}_{\sigma\sigma}&\boldsymbol{U}^{(2)}_{\sigma+}\\ \mathbf{0}&\mathbf{0}\end{bmatrix}\\ &+\begin{bmatrix}\boldsymbol{W}_{\sigma-}\\ \mathbf{0}\\ \boldsymbol{R}_-\end{bmatrix}\begin{bmatrix}\boldsymbol{\Psi}^{(2)}_{-\sigma}&\boldsymbol{\Psi}^{(2)}_{-+}\end{bmatrix}=\mathbf{0}\,.\end{aligned}$$

Multiplying the first block by $2\boldsymbol{\Sigma}^{-2}$, we obtain the Sylvester equation:

$$\begin{aligned}&\begin{bmatrix}\boldsymbol{U}^{(1)}_{\sigma\sigma}-2\boldsymbol{\Sigma}^{-2}\boldsymbol{D}&2\boldsymbol{\Sigma}^{-2}\boldsymbol{W}_{\sigma-}\\ \boldsymbol{\Psi}^{(1)}_{-\sigma}&\boldsymbol{R}_-\end{bmatrix}\begin{bmatrix}\boldsymbol{U}^{(2)}_{\sigma\sigma}&\boldsymbol{U}^{(2)}_{\sigma+}\\ \boldsymbol{\Psi}^{(2)}_{-\sigma}&\boldsymbol{\Psi}^{(2)}_{-+}\end{bmatrix}\\ &+\begin{bmatrix}\boldsymbol{U}^{(2)}_{\sigma\sigma}&\boldsymbol{U}^{(2)}_{\sigma+}\\ \boldsymbol{\Psi}^{(2)}_{-\sigma}&\boldsymbol{\Psi}^{(2)}_{-+}\end{bmatrix}\boldsymbol{U}_+^{(1)}+\begin{bmatrix}2\boldsymbol{\Sigma}^{-2}\mu\boldsymbol{I}_M&\mathbf{0}\\ \mathbf{0}&\mathbf{0}\end{bmatrix}=\mathbf{0}\,.\end{aligned}$$

Continuing to solve (38) backwards, we obtain for $k\ge3$:

$$\begin{aligned}&\frac12\begin{bmatrix}\boldsymbol{\Sigma}^2&\mathbf{0}\\ \mathbf{0}&\mathbf{0}\\ \mathbf{0}&\mathbf{0}\end{bmatrix}\sum_{l=1}^k\boldsymbol{U}_+^{(l)}\cdot\boldsymbol{U}_+^{(k+1-l)}\\ &-\begin{bmatrix}\boldsymbol{D}&\mathbf{0}&\mathbf{0}\\ \mathbf{0}&\boldsymbol{I}_+&\mathbf{0}\\ \mathbf{0}&\mathbf{0}&-\boldsymbol{I}_-\end{bmatrix}\sum_{l=1}^k\boldsymbol{\Psi}_+^{(l)}\cdot\boldsymbol{U}_+^{(k+1-l)}+\mathcal{P}(\boldsymbol{\Theta})\cdot\boldsymbol{\Psi}_+^{(k)}=\mathbf{0}\,.\end{aligned}$$

In this iteration, we assume that the matrices with an exponent lower than k are already known. That is why, starting from $k=2$, in each iteration, the only unknown is $\boldsymbol{Z}_+^{(k)}$. Writing out this system yields (40). The results concerning $\boldsymbol{Z}_-^{(k)}$ are obtained analoguously.

Appendix D. Kou's model and exponential death time

Kou's model is obtained as $m=n=1$, $\boldsymbol{V}_{+\sigma}=-\boldsymbol{R}_+=\alpha_+$, $\boldsymbol{V}_{-\sigma}=-\boldsymbol{R}_-=\alpha_-$, $\boldsymbol{W}_{\sigma-}=p\lambda$, $\boldsymbol{W}_{\sigma+}=(1-p)\lambda$ and $\boldsymbol{Q}=-\lambda$.

$$\begin{aligned}&\frac12\begin{bmatrix}\sigma_1^2&0\\0&0\\0&0\end{bmatrix}\left(\boldsymbol{U}_+^{(1)}\right)^2-\begin{bmatrix}d_1&0&0\\0&1&0\\0&0&-1\end{bmatrix}\begin{bmatrix}1&0\\0&1\\ \Psi^{(1)}_{-\sigma}&\Psi^{(1)}_{-+}\end{bmatrix}\boldsymbol{U}_+^{(1)}\\ &+\begin{bmatrix}-\lambda-\mu-\theta^{(1)}&(1-p)\lambda&p\lambda\\ \alpha_+&-\alpha_+&0\\ \alpha_-&0&-\alpha_-\end{bmatrix}\begin{bmatrix}1&0\\0&1\\ \Psi^{(1)}_{-\sigma}&\Psi^{(1)}_{-+}\end{bmatrix}\\ &=\begin{bmatrix}0\\0\\0\end{bmatrix}.\end{aligned}\tag{74}$$

Assume that $\boldsymbol{U}_+^{(1)}$ has an eigenvalue β with corresponding eigenvector $\boldsymbol{w}$ whose first element is (without loss of generality) 1, we obtain for $w_2\in\mathbb{R}$:

$$\begin{aligned}&\left(\begin{bmatrix}\frac12\sigma_1^2\beta^2-d_1\beta&0\\0&-\beta\\ \Psi^{(1)}_{-\sigma}\beta&\Psi^{(1)}_{-+}\beta\end{bmatrix}\right.\\ &\left.+\begin{bmatrix}-\lambda-\mu-\theta^{(1)}+p\lambda\Psi^{(1)}_{-\sigma}&(1-p)\lambda+p\lambda\Psi^{(1)}_{-+}\\ \alpha_+&-\alpha_+\\ \alpha_-(1-\Psi^{(1)}_{-\sigma})&-\alpha_-\Psi^{(1)}_{-+}\end{bmatrix}\right)\begin{bmatrix}1\\w_2\end{bmatrix}\\ &=\begin{bmatrix}0\\0\\0\end{bmatrix}.\end{aligned}\tag{75}$$

We can solve the second line to $w_2=\alpha_+/(\alpha_++\beta)$. Denoting the two eigenvalues of $\boldsymbol{U}_+^{(1)}$ by $(-\beta_1)<(-\beta_2)<0$ (they exist as $\boldsymbol{U}_+^{(1)}$ is a generator matrix), their corresponding eigenvectors relate to unit vectors as follows:

$$-\frac{(\alpha_+ - \beta_1)(\alpha_+ - \beta_2)}{\alpha_+(\beta_2 - \beta_1)}\left(\begin{bmatrix}1\\ \frac{\alpha_+}{\alpha_+-\beta_1}\end{bmatrix} - \begin{bmatrix}1\\ \frac{\alpha_+}{\alpha_+-\beta_2}\end{bmatrix}\right) = \begin{bmatrix}0\\1\end{bmatrix},$$

$$\frac{1}{\beta_2 - \beta_1}\left((\alpha_+ - \beta_1)\begin{bmatrix}1\\ \frac{\alpha_+}{\alpha_+-\beta_1}\end{bmatrix} - (\alpha_+ - \beta_2)\begin{bmatrix}1\\ \frac{\alpha_+}{\alpha_+-\beta_2}\end{bmatrix}\right) = \begin{bmatrix}1\\0\end{bmatrix}.$$

From this, we obtain:

$$\begin{aligned}\boldsymbol{U}_+^{(1)}\begin{bmatrix}0\\1\end{bmatrix} &= -\frac{(\alpha_+ - \beta_1)(\alpha_+ - \beta_2)}{\alpha_+(\beta_2 - \beta_1)}\left((-\beta_1)\begin{bmatrix}1\\ \frac{\alpha_+}{\alpha_+-\beta_1}\end{bmatrix}\right.\\ &\qquad \left. -(-\beta_2)\begin{bmatrix}1\\ \frac{\alpha_+}{\alpha_+-\beta_2}\end{bmatrix}\right)\\ &= \begin{bmatrix}-\frac{\beta_1\beta_2}{\alpha_+} + \beta_1 + \beta_2 - \alpha_+\\ -\alpha_+\end{bmatrix},\\ \boldsymbol{U}_+^{(1)}\begin{bmatrix}1\\0\end{bmatrix} &= \frac{1}{\beta_2 - \beta_1}\left((-\beta_1)(\alpha_+ - \beta_1)\begin{bmatrix}1\\ \frac{\alpha_+}{\alpha_+-\beta_1}\end{bmatrix}\right.\\ &\qquad \left. -(-\beta_2)(\alpha_+ - \beta_2)\begin{bmatrix}1\\ \frac{\alpha_+}{\alpha_+-\beta_2}\end{bmatrix}\right)\\ &= \begin{bmatrix}\alpha_+ - \beta_1 - \beta_2\\ \alpha_+\end{bmatrix}.\end{aligned}$$

Summarizing, we obtain:

$$\boldsymbol{U}_+^{(1)} = \begin{bmatrix}\alpha_+ - \beta_1 - \beta_2 & -\frac{\beta_1\beta_2}{\alpha_+} + \beta_1 + \beta_2 - \alpha_+\\ \alpha_+ & -\alpha_+\end{bmatrix}.$$

The last line in equation (74) reads as $\begin{bmatrix}\Psi_{-\sigma}^{(1)} & \Psi_{-+}^{(1)}\end{bmatrix}\boldsymbol{U}_+^{(1)} - \alpha_-\begin{bmatrix}\Psi_{-\sigma}^{(1)} & \Psi_{-+}^{(1)}\end{bmatrix} + \begin{bmatrix}\alpha_- & 0\end{bmatrix} = \mathbf{0}$, or, equivalently:

$$\begin{bmatrix}\Psi_{-\sigma}^{(1)} & \Psi_{-+}^{(1)}\end{bmatrix}\left(\boldsymbol{U}_+^{(1)} - \begin{bmatrix}\alpha_- & 0\\ 0 & \alpha_-\end{bmatrix}\right) = \begin{bmatrix}-\alpha_- & 0\end{bmatrix} \tag{76}$$

that can be solved as:[10]

$$\begin{aligned}\begin{bmatrix}\Psi_{-\sigma}^{(1)}\\ \Psi_{-+}^{(1)}\end{bmatrix}' &= \begin{bmatrix}-\alpha_- & 0\end{bmatrix}\frac{1}{\det\left(\boldsymbol{U}_+^{(1)} - \begin{bmatrix}\alpha_- & 0\\ 0 & \alpha_-\end{bmatrix}\right)}\\ &\qquad \begin{bmatrix}-\alpha_- - \alpha_+ & \frac{\beta_1\beta_2}{\alpha_+} - \beta_1 - \beta_2 + \alpha_+\\ -\alpha_+ & \alpha_+ - \alpha_- - \beta_1 - \beta_2\end{bmatrix}\\ &= \frac{\alpha_-}{(\beta_1 + \alpha_-)(\beta_2 + \alpha_-)}\begin{bmatrix}\alpha_+ + \alpha_-\\ -\frac{\beta_1\beta_2}{\alpha_+} + \beta_1 + \beta_2 - \alpha_+\end{bmatrix}',\end{aligned}$$

where, in the last step, we have used that $\det(\boldsymbol{U}_+^{(1)}) = \beta_1\beta_2$. We obtain:

$$\begin{bmatrix}\Psi_{-\sigma}^{(1)} & \Psi_{-+}^{(1)}\end{bmatrix}\begin{bmatrix}1\\ \frac{\alpha_+}{\alpha_++\beta}\end{bmatrix} = \frac{\alpha_-}{\alpha_- - \beta}\,. \tag{77}$$

From the first line of (75), we then obtain

$$\begin{aligned}0 &= \frac{1}{2}\sigma_1^2\beta^2 - d_1\beta - \mu - \theta^{(1)} + \lambda\left(p\frac{\alpha_-}{\alpha_- - \beta} + (1-p)\frac{\alpha_+}{\alpha_+ + \beta} - 1\right)\\ &= \boldsymbol{\Psi}(-\beta, \boldsymbol{\Theta}) - \mu = 0\,.\end{aligned}$$

In other words, the eigenvalues β of $\boldsymbol{U}_+^{(1)}$ satisfy $\boldsymbol{\Psi}(-\beta, \boldsymbol{\Theta}) = \mu$ and are thus given by $(-\beta_1)$, $(-\beta_2)$ with $-\beta_2 < -\beta_1 < 0$ and $\boldsymbol{\Theta} = \theta^{(1)}$, see (14) and Example 6.6.

[10] Note that the inverse of a 2×2 matrix is given by:

$$A^{-1} := \begin{bmatrix}a & b\\ c & d\end{bmatrix}^{-1} = \frac{1}{\det(A)}\begin{bmatrix}d & -b\\ -c & a\end{bmatrix}.$$

References

Ai, M., & Zhang, Z. (2022). Pricing some life-contingent lookback options under regime-switching Lévy models. *Journal of Computational and Applied Mathematics*, Article 114082.

Asmussen, S. (2003). *Applied probability and queues*. Springer, New York.

Asmussen, S., & Albrecher, H. (2010). *Ruin probabilities*. Advanced Series on Statistical Science & Applied Probability, Vol. 14.

Asmussen, S., Laub, P. J., & Yang, H. (2019). Phase-type models in life insurance: Fitting and valuation of equity-linked benefits. *Risks, 7*(1), 1–17.

Ballotta, L., Deelstra, G., & Rayée, G. (2017). Multivariate FX models with jumps: Triangles, quantos and implied correlation. *European Journal of Operational Research, 260*, 1181–1199.

Bauer, D., Reuss, A., & Singer, D. (2012). On the calculation of the solvency capital requirement based on nested simulations. *ASTIN Bulletin, 42*(2), 453–499.

Benth, F. E., Deelstra, G., & Kozpinar, S. (2021). Pricing energy quanto options in the framework of markov-modulated additive processes. *IMA Journal of Management Mathematics, 34*(1), 187–220.

Bowers, N. L., Gerber, H. U., Hickman, J. C., Jones, D. A., & Nesbitt, C. J. (1997). *Actuarial mathematics*. Society of Actuaries, Schaumburg, Illinois.

Breuer, L. (2008). First passage times for Markov additive processes with positive jumps of phase type. *Journal of Applied Probability, 45*(3), 779–799.

Brigo, D., & Vrins, F. (2018). Disentangling wrong-way risk: Pricing credit valuation adjustment via change of measures. *European Journal of Operational Research, 269*(3), 1154–1164.

Buffington, J., & Elliott, R. J. (2002). American options with regime switching. *International Journal of Theoretical and Applied Finance, 5*, 497–514.

Cai, N., & Kou, S. G. (2011). Option pricing under a mixed-exponential jump diffusion model. *Management Science, 57*(11), 2067–2081.

Cai, N., Song, Y., & Kou, S. (2015). A general framework for pricing Asian options under Markov processes. *Operations Research, 63*(3), 540–554.

Carr, P. (1998). Randomization and the American put. *Review of Financial Studies, 11*(3), 597–626.

Carr, P., & Madan, D. B. (1999). Option valuation using the fast Fourier transform. *Journal of Computational Finance, 2*, 61–73.

Cui, Z., Kirkby, J. L., & Nguyen, D. (2017). Equity-linked annuity pricing with cliquet-style guarantees in regime-switching and stochastic volatility models with jumps. *Insurance: Mathematics & Economics, 74*, 46–62.

Cui, Z., Kirkby, J. L., & Nguyen, D. (2019). A general framework for time-changed Markov processes and applications. *European Journal of Operational Research, 273*(1), 785–800.

Deelstra, G., Latouche, G., & Simon, M. (2020). On barrier option pricing by Erlangization in a regime-switching model with jumps. *Journal of Computational and Applied Mathematics, 371*, Article 112606.

Dong, Y., Lv, W., & Wu, S. (2019). First passage time under a regime-switching jump-diffusion model and its application in the valuation of participating contracts. *Bulletin of the Korean Mathematical Society, 56*(5), 1355–1376.

Elias, R. S., Wahab, M. I. M., & Fang, L. (2014). A comparison of regime-switching temperature modeling approaches for applications in weather derivatives. *European Journal of Operational Research, 232*, 549–560.

Elliott, R. J., Chan, L., & Siu, T. K. (2005). Option pricing and Esscher transform under regime switching. *Annals of Finance, 1*(4), 423–432.

Eustice, D., & Klamkin, M. S. (1979). On the coefficients of a partial fraction decomposition. *American Mathematical Monthly, 86*(6), 478–480.

Feng, R., Gan, G., & Zhang, N. (2022). Variable annuity pricing, valuation, and risk management: A survey. *Scandinavian Actuarial Journal, 10*(1–34), 867–900.

Gardiner, J. D., Laub, A. J., Amato, J. J., & Moler, C. B. (1992). Solution of the Sylvester matrix equation $AXB^T + CXD^T = E$. *ACM Transactions on Mathematical Software, 18*(2), 232–238.

Gerber, H. U., Shiu, E. S. W., & Yang, H. (2012). Valuing equity-linked death benefits and other contingent options: A discounted density approach? *Insurance: Mathematics and Economics, 51*, 73–92.

Gerber, H. U., Shiu, E. S. W., & Yang, H. (2013). Valuing equity-linked death benefits in jump diffusion models. *Insurance: Mathematics & Economics, 53*, 615–623.

Gerber, H. U., Shiu, E. S. W., & Yang, H. (2015). Geometric stopping of a random walk and its applications to valuing equity-linked death benefits. *Insurance: Mathematics and Economics, 64*, 313–325.

Godin, F., & Trottier, D. A. (2019). Option pricing under regime-switching models: Novel approaches removing path-dependence. *Insurance: Mathematics and Economics, 87*, 130–142.

Hainaut, D. (2014). Impulse control of pension fund contributions, in a regime switching economy. *European Journal of Operational Research, 239*, 1024–1042.

Hamilton, J. D. (1989). A new approach to the economic analysis of nonstationary time series and the business cycle. *Econometrica, 57*(2), 357–384.

Hassanzadeh, H., & Pooladi-Darvish, M. (2007). Comparison of different numerical laplace inversion methods for engineering applications. *Applied Mathematics and Computation, 189*(2), 1966–1981.

Hieber, P. (2014). First-passage times of regime switching models. *Statistics & Probability Letters, 92*, 148–157.

Hieber, P. (2017). Cliquet-style return guarantees in a regime-switching Lévy model. *Insurance: Mathematics & Economics, 72*, 138–147.

Hieber, P. (2018). Pricing exotic options in a regime switching economy: a Fourier transform method. *Review of Derivatives Research, 21*(2), 231–252.

Hieber, P., & Scherer, M. (2010). Efficiently pricing barrier options in a Markov-switching framework. *Journal of Computational and Applied Mathematics, 235*, 679–685.

Hieber, P., & Scherer, M. (2012). A note on first-passage times of continuously time-changed Brownian motion. *Statistics & Probability Letters, 82*(1), 165–172.
Huang, J., Zhu, W., & Ruan, X. (2014). Option pricing using the fast Fourier transform under the double exponential jump model with stochastic volatility and stochastic intensity. *Journal of Computational and Applied Mathematics, 263*, 152–159.
Ivanovs, J. (2010). Markov-modulated Brownian motion with two reflecting barriers. *Journal of Applied Probability, 47*(4), 1034–1047.
Jiang, Z., & Pistorius, M. R. (2008). On perpetual American put valuation and first–passage in a regime-switching model with jumps. *Finance and Stochastics, 12*(3), 331–355.
Jin, Z., Liu, G., & Yang, H. (2020). Optimal consumption and investment strategies with liquidity risk and lifetime uncertainty for Markov regime-switching jump diffusion models. *European Journal of Operational Research, 280*, 1130–1143.
Jin, Z., Qian, L., Wang, W., & Yang, R. (2016). Pricing dynamic fund protections with regime switching. *Journal of Computational and Applied Mathematics, 297*, 13–25.
Kijima, M., & Siu, C. C. (2014). On the first passage time under regime-switching with jumps. *Inspired by Finance: The Musiela Festschrift*, 387–410.
Kirkby, J. L. (2023). Hybrid equity swap, cap, and floor pricing under stochastic interest by markov chain approximation. *European Journal of Operational Research, 305*(2), 961–978.
Kirkby, J. L., & Nguyen, D. (2021). Equity-linked guaranteed minimum death benefits with dollar cost averaging. *Insurance: Mathematics and Economics, 100*, 408–428.
Korn, R., Melnyk, Y., & Seifried, F. T. (2017). Stochastic impulse control with regime-switching dynamics. *European Journal of Operational Research, 260*, 1024–1042.
Kou, S. G., & Wang, H. (2003). First passage times of a jump diffusion process. *Advances in Applied Probability, 35*(2), 504–531.
Le Courtois, O., Quittard-Pinon, F., & Su, X. (2020). Pricing and hedging defaultable participating contracts with regime switching and jump risk. *Decisions in Economics and Finance, 43*(1), 303–339.
Liang, X., Tsai, C. C.-L., & Lu, Y. (2016). Valuing guaranteed equity-linked contracts under piecewise constant forces of mortality. *Insurance: Mathematics & Economics, 70*, 150–161.
Mijatović, A., & Pistorius, M. (2011). Exotic derivatives under stochastic volatility models with jumps. In *Advanced mathematical methods for finance* (pp. 455–508). Springer.
Nguyen, G., & Poloni, F. Componentwise accurate Brownian motion computations using Cyclic Reduction. arXiv:1605.01482
Robert, S., & Boudec, J. Y. (1997). New models for pseudo self-similar traffic. *Performance Evaluation, 30*, 57–68.
Rogers, L. C. G. (1994). Fluid models in queueing theory and Wiener-Hopf factorization of Markov chains. *Annals of Applied Probability, 4*(2), 390–413.
Scarf, P. A., Cavalcante, C. A. V., & Lopes, R. S. (2019). Delay-time modelling of a critical system subject to random inspections. *European Journal of Operational Research, 278*(3), 772–782.
Siu, C. C., Yam, C. P., & Yang, H. (2015). Valuing equity-linked death benefits in a regime-switching framework. *ASTIN Bulletin, 45*(2), 355–395.
Sylvester, J. J. (1883). On the equation to the secular inequalities in the planetary theory. *Philosophical Magazine Series, 5*, 267–269.
Wang, Y., Zhang, Z., & Yu, W. (2021). Pricing equity-linked death benefits by complex Fourier series expansion in a regime-switching jump diffusion model. *Applied Mathematics and Computation, 399*, Article 126031.
Zhang, Z., & Su, W. (2018). A new efficient method for estimating the Gerber-Shiu function in the classical risk model. *Scandinavian Actuarial Journal, 2018*(5), 426–449.
Zhang, Z., & Yong, Y. (2019). Valuing guaranteed equity-linked contracts by Laguerre series expansion. *Journal of Computational and Applied Mathematics, 357*, 329–348.
Zhang, Z., Yong, Y., & Yu, W. (2021). Valuing equity-linked death benefits in general exponential Lévy models. *Journal of Computational and Applied Mathematics, 365*, Article 112377.